

February 27, 2017

Natascha Töpfer  
Copernicus Publications  
Editorial Support  
[editorial@copernicus.org](mailto:editorial@copernicus.org)

Subject:

Journal: HESS

Title: Hydrological modeling of the Peruvian-Ecuadorian Amazon basin using GPM-IMERG satellite-based precipitation dataset

Author(s): Ricardo Zubieta et al.

MS No.: hess-2016-656

MS Type: Research article

Iteration: Revision

Dear Ms. Töpfer

I am writing in response to you revision regarding the above-mentioned manuscript.

I have received comments and suggestions from two reviewers, which I already gave an answer point-by-point. I would like to thank the referees for their useful comments and for their positive evaluation of this manuscript. According to this, some paragraphs, tables and figures were modified and improved in the revised version. Technical aspects and answers are explained in detail, these can be found in “author comments” section of the “Interactive discussion”:

<http://www.hydrol-earth-syst-sci-discuss.net/hess-2016-656/#discussion>

In general, the comments and suggestion from reviewers have allowed improving the manuscript. Our manuscript was reviewed again, including a grammatical revision, and it has been uploading to the HESSD web site. We hope that this updated version of the manuscript is suitable for publication in HESS Journal.

Thank you very much for your cooperation.

Kind regards,

Ricardo Zubieta  
Geophysical Institute of Peru  
<http://www.met.igp.gob.pe/personal/rzubieta/>

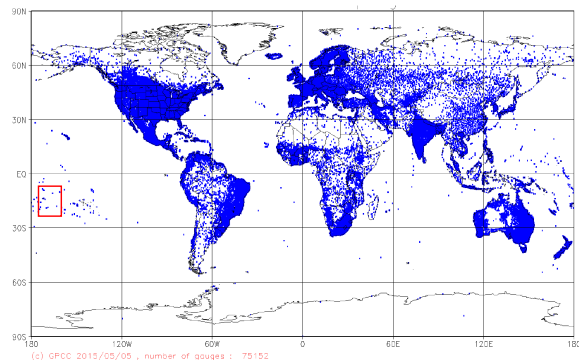
**We would like to thank the referee (1) for his useful comments. Please find below our answers.**

1. P.3 L.22: item b: Does this dataset (TMPA-V7) include information from the rain gauges shown in Fig.1 (all of them, half of them, just a few of them, none of them?). The authors note that TMPA-v7 and GPM-IMERG are the most similar...can the authors discuss a bit why this is so? I assume they use much of the same satellite and rain gauge data...?

GPM is an international US/Japanese Earth science mission involving NASA and JAXA, respectively. The GPM mission improved and expanded on TRMM. GPM and TRMM provide precipitation data derived from different passive microwave (PMW) sources used in IMERG and TMPA, respectively [Huffman et al. 2015], including: Sounder for Atmospheric Profiling of Humidity in the Intertropics by Radiometry (SAPHIR), Advanced Technology Microwave Sounder (ATMS), Atmospheric Infrared Sounder (AIRS), Cross-Track Infrared Sounder (CRIS), and TRMM Combined Instrument (TCI) algorithms (2B31). They also include TRMM Microwave Image (TMI, data ended on 8 Apr 2015), GPM Microwave Imager (GMI), Advanced Microwave Scanning Radiometer for Earth Observing Systems (AMSR-E), Special Sensor Microwave Imager/Sounder (SSMIS), Microwave Humidity Sounder (MHS), Special Sensor Microwave Imager (SSM/I), Advanced Microwave Sounding Unit (AMSU), Operational Vertical Sounder (TOVS) and microwave-adjusted merged geo-infrared (IR).

TMPA 3B42 version 7 is obtained from the preprocessing of data provided by different satellite-based sensors between 1998 and April 2015, in both real and near-real time (TMPA 3b42 data are available at <ftp://disc2.nascom.nasa.gov/data/TRMM/Gridded/3B42RT>). The 3B42 algorithm (every three hours) combines precipitation estimates from TMI, AMSR, SSMIS, SSM/I, AMSU, MHS, TCI, *MetOp-B* and IR. After the preprocessing is complete, the 3-hourly multi-satellite estimations are summed for the month and combined with monthly rainfall obtained from Global Precipitation Climatology Centre (GPCC), which uses ground-based precipitation. The last step is to scale each 3-hourly rainfall estimate for the month to sum to the monthly value (for each pixel separately, 0.25-degree by 0.25-degree spatial resolution).

Both TMPA and GPM-IMERG adopt the Global Precipitation Climatology Centre (GPCC) monthly rain gauge analysis (Huffman et al. 2014). The Monitoring Product is represented on internationally exchanged meteorological data i.e. gauge observations from world-wide 6,000 to 7,000 stations (see next figure, (Schneider et al., 2014). The average gauge density is about 2 gauges per 2.5° by 2.5° lat/long grid box only. Building upon the figure of rainfall stations and lat/long grid (Schneider et al., 2015), it very probably that 105 rainfall stations used in our study were considered by GPCC calculations.



*Spatial distribution of monthly in-situ stations with a climatological precipitation normal,*

*based on at least 10 years of data in GPCC data base (Schneider et al., 2014)*

Huffman, G.J., Bolvin, D.T., Nelkin, E.J.: Day 1 IMERG Final Run Release Notes; NASA Goddard Earth Sciences Data and Information Services Center: Greenbelt, MD, USA, 2015.

Schneider, U., Becker, A., Finger, P. et al. GPCC's new land surface precipitation climatology based on quality-controlled in situ data and its role in quantifying the global water cycle. *Theor Appl Climatol* (2014) 115: 15. doi:10.1007/s00704-013-0860-x

2. P.3 L.5: Two questions related to details: could the observed rainfall have been interpolated to a 0.25x0.25 grid for better comparison with the TMPA data sets? 0.15x0.15 for the GPM-IMERG dataset? And in regions of mountainous terrain, oftentimes consideration of the altitude-rainfall gradient relationship is critical for spatially distributing rainfall onto a grid. Was this information included in the interpolation? Do the authors think this effect is important in this region?

Initially, observed rainfall was interpolated for 0.5°\*0.5°, 0.25°\*0.25° and 0.15°\*0.15° grids (without significant changes in the rainfall analysis or hydrological model performance). Nonetheless, not to lose more detailed spatial information a 0.10°\*0.10° grid over Andean regions (in this paper greater than 1500 masl) was selected for the interpolation process, since there are more rainfall stations close to each other over Andean regions than Amazon regions (in this paper, region lower than 1500 masl).

3. P.4 L.9: MGB uses the rainfall aggregated to a daily time step. So, it seems that one of the main possible advantages of the GPM-IMERG (30 minute time step) dataset compared to the TMPA-V7 (3 hourly) for computing runoff generation by MGB is lost, especially since the convective nature of the rainfall is likely better resolved, in theory at least, using a 30 minute time step. Is there anything in MGB that can take advantage of the diurnal temporal distribution of the rainfall? If not, I think the authors should at least comment that hydrological models using sub-diurnal time steps might have larger differences between the TMPA and GPM-IMERG datasets owing to their different temporal resolutions...Can the authors comment on this?

Thank you for your comment

The improvements in MGB-IPH software do not currently include topics about sub-daily time step (<https://www.ufrgs.br/hge/mgb-iph/>).

In general, the performance of the model when using GPM-IMERG datasets indicates that these data are useful for estimating observed streamflows in Andean-Amazonian regions (Ucayali basin, southern regions of the Peruvian and Ecuadorian Amazon Basin). These results are similar to those obtained from TMPA V7 estimates by Zubieta et al. [2015] for the 2003-2009 period. Streamflows obtained from GPM-IMERG, TMPA V7, TMPA RT datasets show the same spatial pattern as those obtained by using PLU, (low and high performance in the northern and southern regions of the ABPE, respectively). The ability to represent seasonal streamflows in the southern region using these four precipitation datasets is validated with statistical evaluation.

It is important to note that advantages of GPM-IMERG compared to the TMPA-V7, such as the temporal resolution (30 minutes against 3 hours, respectively), for estimating streamflows have not yet been fully analyzed. The use of sub-daily rainfall data is potentially interesting to simulate discharge variability in the Andean rivers, where short convective rainfall episodes are more relevant for hydrological variability. In this study, precipitation and streamflows were analyzed at the daily time step. Further flash flood modeling at smaller scales would be able to evidence the effects of sub-diurnal differences between datasets

Zubieta, R., Geritana, A., Espinoza, J.C. and Lavado W.: Impacts of Satellite-based Precipitation Datasets on Rainfall-Runoff Modeling of the Western Amazon Basin of Peru and Ecuador, *Journal of Hydrology*, doi:10.1016/j.jhydrol.2015.06.064, 2015.

4. P.5 L.1: How were these thresholds selected? Are they based on some sort of statistical analysis?

The Amazon basin of Perú and Ecuador can present different rainfall regimes (Espinoza et al., 2009; Laraque et al., 2007). Rainfall thresholds for the initiation of events such as landslides or floods can be variable in

space and time, for example, extreme rainfall (amount) in one Andean region may be normal in Amazon region. In this study, those thresholds are obtained from frequency analysis (percentiles 5, 20, 60, 90, 95).

Espinoza, J.C, Ronchail, J., Guyot, J.L., Cochonneau, G., Filizola, N.P., Lavado, C., De Oliveira, E., Pombosa, R., Vauchel P.: Spatio-Temporal rainfall variability in the Amazon basin countries (Brazil, Peru, Bolivia, Colombia and Ecuador), *I.J. of Climatology* 29(11): 1574–1594, doi:10.1002/joc.1791, 2009.

Laraque, A., Ronchail, J., Cochonneau, G., Pombosa, R., Guyot, J.L.: Heterogeneous distribution of rainfall and discharge regimes in the Ecuadorian Amazon basin, *Journal of Hydrometeorology* 8: 1364–1381, doi:10.1175/2007JHM784.1, 2007.

5. P.5 L.25: The text “overestimate observations”...should likely be modified to something like “produce overestimates compared to observations”.

Thank you so much, that would be considered:

Total annual rainfall over the ABPE during the selected period is shown in Figs. 1c-f, using all four precipitation products. The satellite-based datasets (GPM-IMERG, TMPA V7 and TMPA RT) produce overestimates compared to observations (PLU) during this period (by 11.1%, 15.7% and 27.7 %, respectively).

6. P.6 L.10-11: The authors have reported that the satellite-based datasets underestimate the dry and wet season rainfall much more for the Huallaga basin compared to the Ucayali basin: do the authors have any insights as to why this is?

The Huallaga basin is not predominantly an Amazon region as is the Ucayali basin. The Andean region (higher than 1500 msal) is more present in the Huallaga basin (51%) than Ucayali basin (39%). The limitations to represent adequate rainfall from the satellite-based precipitation can be due to the strong spatial variability of rainfall in the Amazon-Andes region. Our finding about predominant underestimation in relation to observed rainfall along the Huallaga basin is consistent with others research developed over Andean regions of Peru (Condom et al, 2010), Bolivia (Scheel et al., 2011) and Ecuador ( Zulkafli et al., 2014).

Condom, T., Rau, P., Espinoza, J.C. 2011. Correction of the TRMM 3B43 monthly precipitation data over the mountainous areas of Peru during the period 1998–2007. *Hydrological Processes*. DOI: 10.1002/hyp.7949.

Scheel, M. L. M., Rohrer, M., Huggel, Ch., Santos Villar, D., Silvestre, E., and Huffman, G. J. 2011. Evaluation of TRMM Multi-satellite Precipitation Analysis (TMPA) performance in the Central Andes region and its dependency on spatial and temporal resolution, *Hydrol. Earth Syst. Sci.*, 15, 2649-2663, doi:10.5194/hess-15-2649.

Zulkafli, Z., Buytaert, W., Onof, C., Manf, B., Tarnavsky, E., Lavado, W., and Guyot, J. L. 2014. A Comparative Performance Analysis of TRMM 3B42 (TMPA) Versions 6 and 7 for Hydrological Applications over Andean–Amazon River Basins. *J. Hydrometeor.*, 15, 581–592, DOI: 10.1175/JHM-D-13-094.1

7. P.6 L.18-20: While I am not surprised that detection of light events was difficult, why do the products have such difficulty predicting strong rainfall events? I might have (perhaps erroneously or naively I admit) assumed that such events might be better detected. Can the authors comment on this? For example, are the strongest events occurring in high altitude/mountainous regions which are more difficult to detect? Is the smoothing to daily averages related to this problem?

Thank you for the suggestion, these paragraphs would be considered in the manuscript

High or extreme precipitation events can be variable in space and time, rainfall amount for extreme events in one Andean mountain may be normal in Amazon region. This limitation to represent adequate rainfall from the satellite-based precipitation can be due to the strong spatial variability of rainfall in the Amazon-Andes region. Indeed, the AB is distinguished by complex rainfall spatial distribution from the interactions between topography and large-scale humidity transport [Espinoza et al., 2015].

Assessment of rainfall estimates (GPM-IMERG, TMPA V7 and TMPA RT) with respect to PLU have been also performed using the Heidke Skill Score (HSS). HSS is a measure of skill in predictions, classified as below normal, near-normal and above-normal (Wilks, 1995). The assesment from HSS is based on the number of correctly predicted data where the category with the largest probability turns out to be correct. As reflected in the formula:  $HSS = \frac{C-E}{N-E}$ , where C is the number of correct predictions, E is the number of correct predictions expected by chance and N is the total number of predictions. HSS = 1 refers to a perfect prediction, HSS = 0 shows no skill and HSS < 0, indicates that a prediction is worse than a random prediction.

The HSS spatial distribution estimated from daily precipitation using each satellite dataset (GPM-IMERG, TMPA V7 and TMPA RT) and PLU was calculated using thresholds (0.1, 1, 5, 10 and 20 mm/day) as a reference prediction (Fig. S3a-c). In general, for the daily scale, the HSS score varies between 0 and 0.4, indicating low skill. The mean HSS for GPM-IMERG shows a moderate HSS score of around 0.4 in the Northern region (Fig. S3a). The lowest HSS values (lower than 0.2) for GPM-IMERG are mainly located in the Andean regions, where there are more rainfall stations than in the Amazonian regions. This could be due to strong spatial variability, which is characterized by rainfall decrease with altitude and by the leeward or windward position of the stations (Espinoza et al, 2009). Low scores are also observed in more scattered areas along the ABPE when TMPA V7 and TMPA RT are analyzed (lower than 0.15). Nevertheless, this relationship is slightly improved in the northern region of the Ucayali basin (~0.2).

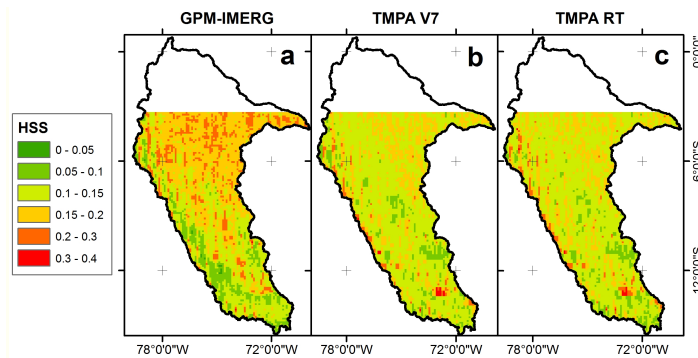


Fig. S3. Spatial variability of the Heidke Skill Score from a) GPM-IMERG, b) TMPA V7 and c) TMPA RT against PLU ground observation, period from 2014 to 2015.

Espinoza, J. C., Chavez, S, Ronchail, J., Junquas, C., Takahashi, K. and Lavado, W., 2015. Rainfall hotspots over the southern tropical Andes: Spatial distribution, rainfall intensity, and relations with large-scale atmospheric circulation. *Water Resour. Res.* 51, 3456-3475.

8. P.7 L.3: The calibration is glossed over a bit it seems: what set of parameters were calibrated? Were parameters calibrated separately for each precipitation dataset? Also, no information is given on the quality or calibration of the MGB evaporation. Is it significant compared to the rainfall? Are there non-negligible compensating errors (evaporation bias might offset rainfall or discharge errors/biases)? A short discussion is needed.

To optimize the simulation of streamflows from precipitation datasets, different parameter sets were assigned to each basin in the ABPE during calibration. Analysis by sub-basin is more reliable than assigning the same parameter set to the entire basin [Zubieta et al., 2015]. Based on sensitivity analysis of the MGB-IPH model [Collischonn et al., 2007] six parameters were selected for calibration:  $Wm_i$  (mm),  $b_1$  (-),  $Kint$  (mm.d<sup>-1</sup>),

$Kbas_i$  ( $\text{mm} \cdot \text{d}^{-1}$ ),  $CS_i$  (-) and  $CI_i$  (-), where  $Wm$  represents water retained in the soil, which influences the evaporation process over time;  $Kint$  and  $Kbas$  control the amount of water in cases in which subsurface soil and groundwater, respectively, are saturated; and  $CS$  and  $CI$  allow for adjustment of retention time of flows [Collischonn et al., 2007]. To determine optimal parameters, an automatic calibration process was used in order to reduce the domain extent; a previous manual adjustment of the values was performed. To ensure impartiality, parameter sets were calibrated separately for each precipitation dataset. For each parameter value, different domains were considered initially, in which a first value determined by manual calibration was defined as the relative centroid for each domain. The MOCOM-UA multi-criteria global optimization algorithm [Yapo et al., 1998] was then used to find optimal solutions for six parameters. This process results in an effective and efficient search on the Pareto optimum space [Boyle et al., 2000]. To analyze the impacts on the calibrated parameters, average parameters were calculated for precipitation datasets and HRU (Table 4).

The results of the calibration process indicate that overestimation by TMPA RT compared to observed rainfall (PLU), GPM-IMERG and TMPA V7 (Fig. 2a) in several months is consistent with a mean increase in  $Wm$  (+53%, +6%, +15% respectively), along with a predominantly mean decrease in  $Kbas$  (-18%, -39% and -16% respectively) and  $Kint$  (-25%, -15%, +2%) to achieve water balance (Table 4). Meanwhile, the overestimation by PLU compared to GPM-IMERG, TMPA V7 and TMPA RT (Fig. 3a) is consistent with a mean increase in  $Wm$  (+33%, +38%, +34% respectively), along with a mean decrease in  $Kbas$  (-30%, -28% and -38% respectively) and  $Kint$  (-17%, -16%, -17%) to achieve water balance (Table 4).

Table 3. Model parameters subjected to the process of automatic calibration for the Peruvian and Ecuadorian Amazon basin.

Parameter	HRU	Hydrological process	First guess	Domain
$Wm(\text{mm})$	Shrubs, agricultural areas/not deep soils	Water storage on the HRU	200	50-1200
	Shrubs, agricultural areas/deep soils		400	50-1200
	Forest/not deep soils		350	50-1200
	Forest/deep soils		600	50-1200
	Pasture/not deep soils		120	50-1200
	Pasture/deep soils		240	50-1200
$Kint(\text{mm}/\text{d})$	Shrubs, agricultural areas/not deep soils	Sub - surface flow	80	50-150
	Shrubs, agricultural areas/deep soils		90	50-150
	Forest/not deep soils		100	50-150
	Forest/deep soils		120	50-150
	Pasture/not deep soils		70	50-150
	Pasture/deep soils		80	50-150
$Kbas(\text{mm}/\text{d})$	Shrubs, agricultural areas/not deep soils	Groundwater flow	30	10 - 100
	Shrubs, agricultural areas/deep soils		50	10 - 100
	Forest/not deep soils		70	10 - 100
	Forest/deep soils		80	10 - 100
	Pasture/not deep soils		55	10 - 100
	Pasture/deep soils		70	10 - 100
$CS$	All	Surface flow	15	0.35 - 40
$CI(-)$	All	Sub-surface flow	120	1 - 200
$b(-)$	All	Variable infiltration curve	0.12	0.01 - 2

Table 4. Values of the model mean parameters used in the *Ucayali and Huallaga basins for each rainfall datasets for the 2014-2015 period.*

Parameter	HRU	UCAYALI BASIN				HUALLAGA BASIN			
		PLU	GPM- IMERG	TMPA V7	TMPA RT	PLU	GPM- IMERG	TMPA V7	TMPA RT
Wm(mm)	Shrubs, agricultural areas/not deep soils	268	351	294	373	100	60	65	60
	Shrubs, agricultural areas/deep soils	340	472	503	597	132	102	96	99
	Forest/not deep soils	300	408	273	344	130	101	99	96
	Forest/deep soils	422	453	445	435	250	203	180	209
	Pasture/not deep soils	144	350	261	321	101	60	66	59
	Pasture/deep soils	196	400	454	496	150	120	116	121
Kint (mm/d)	Shrubs, agricultural areas/not deep soils	141	216	151	151	190	161	163	152
	Shrubs, agricultural areas/deep soils	180	236	156	163	220	189	195	198
	Forest/not deep soils	198	123	107	108	103	162	155	160
	Forest/deep soils	200	134	108	113	120	208	199	220
	Pasture/not deep soils	150	110	119	122	121	160	151	150
	Pasture/deep soils	180	113	126	128	132	193	201	190
Kbas (mm/d)	Shrubs, agricultural areas/not deep soils	103	121	89	93	55	70	72	80
	Shrubs, agricultural areas/deep soils	113	123	100	103	61	90	94	100
	Forest/not deep soils	53	134	59	53	44	70	69	80
	Forest/deep soils	62	25	69	62	63	90	88	100
	Pasture/not deep soils	64	112	66	64	46	70	76	80
	Pasture/deep soils	74	113	71	71	63	90	66	100
CS	All	18	16	17	17	2.6	2.4	2.6	2.5
CI(-)	All	112	111	118	111	111	133	135	132
b(-)	All	0.13	0.17	0.15	0.12	0.12	0.15	0.14	0.14

Yapo, P.O., Gupta, H.V., Sorooshian, S.: Multi-objective global optimization for hydrologic models. *Journal of Hydrology* 204, 83–97, 1998.

Boyle, D.P., Gupta, H.V., Sorooshian, S.: Toward improved calibration of hydrologic models: combining the strengths of manual and automatic methods. *Water Resources Research* 36 (12), 3663–3674, 2000.

Collischonn, W., Allasia, D.G., Silva, B.C., Tucci, C.E.M.: The MGB-IPH model for large-scale rainfall-runoff modeling. *J. Hydrol. Sci.* 52, 878–895, doi: 10.1623/hysj.52.5.878, 2007.

9. P.9 L.8-9: The authors state that seasonal streamflows in the southern region are well modeled using the satellite datasets, and indeed the results support this conclusion. But in the northern part of the Western Amazon basin/region, the results seem to indicate that satellite products are not useful for obtaining streamflows from hydrological modeling: so this implies that further progress is still required.. It think this should also be stated in the conclusions.

Thank you so much, this paragraph would be included

In general, the performance of the model when using the GPM-IMERG dataset indicates that these data are useful for estimating observed streamflows in Andean-Amazonian regions (Ucayali basin, southern regions of the Peruvian and Ecuadorian Amazon Basin). These results are similar to those obtained from TMPA V7 estimates by Zubieta et al. [2015] for the 2003-2009 period. Streamflows obtained from the GPM-IMERG, TMPA V7 and TMPA RT datasets show the same spatial pattern as those obtained by using PLU (low and high performance in the northern and southern regions of the ABPE, respectively). The ability to represent seasonal streamflows in the southern region using these four precipitation datasets is validated with statistical evaluation. Low performance of the model identified in the northern region is mainly related to the lack of adequate rainfall estimates, because it is consistent with estimated streamflows, so this implies that further progress is still required in satellite estimates of rainfall.

Zubieta, R., Geritana, A., Espinoza, J.C. and Lavado W.: Impacts of Satellite-based Precipitation Datasets on Rainfall-Runoff Modeling of the Western Amazon Basin of Peru and Ecuador, *Journal of Hydrology*, doi:10.1016/j.jhydrol.2015.06.064, 2015.

10. P.9 L2.: A 20% detection rate seems low. Can the authors put this into some sort of context for the reader (e.g. is 20% indeed a reasonable value in this region, or would one hope to have 50% or a higher value?). Also, what are the implications of these statistics and their impact on the MGB model simulations? Can a lower, say 10% detection rate, be assumed to be able to produce reasonable Nash scores? Or perhaps there is no clear relationship between these scores and the modeled discharge quality? This is not clear. Can the authors comment on this?

Thank you, a paragraph would be included in manuscript

Analysis of rain events from pixel value comparing PLU and estimated daily rainfall (GPM-IMERG, TMPA V7 and TMPA RT) suggests a low capacity for detection. This does not imply that they are not useful for hydrological modeling, because rain events not correctly detected for a region or a day could be correctly detected on another day or in nearby regions, compensating for the estimation of rainfall amount over large regions.

11. P10 L.15-19: In Fig.4d, it is seen that the poorest Nash scores are in the northern part of the region shown: looking at Fig.4a (or Fig.1b), we see that there are relatively few observations in this region. But, this is where one would hope to benefit the most from a satellite product, but it seems this is not the case. In L.15-19 it is stated that such products hold promise for operational applications in data sparse regions, but it doesn't seem to be the case here? Can the authors comment a bit more or perhaps modify this slightly (seemingly) over-optimistic text?

I am sorry, you are right. The comment would be modified

Their usefulness in Andean-Amazon basins and their applicability as input to hydrological models have been evaluated recently by comparing modeled and observed datasets. Results indicate that these datasets could be used for operational applications in some Andean-Amazon *regions* [Zulkafli et al., 2014; Zubieta et al., 2015]. However, hydrological modeling using satellite-based precipitation data does not yield successful results in equatorial regions. This is mainly because of inadequate satellite estimates, because streamflows resulting from hydrological modeling using observed rainfall show acceptable performance in the Napo River basin in the equatorial region [Zubieta et al., 2015].

Zubieta, R., Geritana, A., Espinoza, J.C. and Lavado W.: Impacts of Satellite-based Precipitation Datasets on Rainfall-Runoff Modeling of the Western Amazon Basin of Peru and Ecuador, *Journal of Hydrology*, doi:10.1016/j.jhydrol.2015.06.064, 2015.

Zulkafli, Z., Buytaert, W., Onof, C., Manf, B., Tarnavsky, E., Lavado, W., and Guyot, J. L.: A Comparative Performance Analysis of TRMM 3B42 (TMPA) Versions 6 and 7 for Hydrological Applications over Andean-Amazon River Basins, *J.Hydrometeor.*, 15, 581–592, doi: 10.1175/JHM-D-13-094.1, 2014.

**We would like to thank the referee (2) for his useful comments.  
Please find bellow our answers.**

Scarcity of the rain gauge network and impact on the comparison results The authors had to work with a very scarce and unevenly spread network – (scarcity which makes satellite information all the more attractive) . They acknowledge briefly that the small number of gauges in part of the basin might explain the discrepancies between the sat/ground rainfall products and between the simulated/observed discharge , but there is no attempt to quantify the uncertainty in the ground rainfall product.

1. the authors should elaborate on the ability of their ground rainfall product PLU to reproduce the rainfall gradients in the mountaneous part of the basins. Is altitude taken into account in their interpolation method and if yes how and was the quantitative uncertainty assessed ? - Also as kriging provides the estimation variance, the authors could provide a map showing the expected quality of the ground product (for instance ratio of kriging std over rainfall estimate for one day or an average over the season)

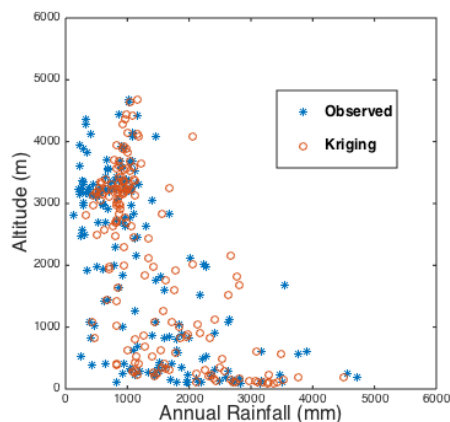


Figure S1.a) Relationship between altitude (m asl) and the observed and interpolated (kriging-PLU) annual rainfall (mm) for the 181 stations of the Peruvian and Ecuadorian Amazon basin for the 2014-2015 period.

To evaluate the ability of PLU to reproduce rainfall gradients in the Andes, the relationship between annual rainfall and altitude for 181 stations was compared. In this area, 100 rainfall station are located above 2000 m asl; some record in excess of 1500 mm/year, while less than 1200 mm/year is generally recorded above 3000 m asl. At lower elevations, abundant rainfall is associated with warm, moist air and the release of a large quantity of water vapor over the first eastern slope of the Andes; as a result, the amount of rainfall decreases with altitude (Laraque et al., 2007; Espinoza et al., 2009). A group of 15 observed rainfall stations located above 2000 m asl shows rainfall amount below 450 mm/year; this group cannot be adequately represented by PLU. Despite these differences, PLU and observed average rainfall show similar behavior at similar altitudes (Fig. S1). Indeed, the observed average rainfall for 181 stations shows high correlation with PLU for the 2014-2015 period ( $r = 0.77$   $p < 0.01$ ) (Fig. S2a). In contrast, observed average rainfall shows lower correlation with GPM-IMERG, TMPA V7 and TMPA RT (0.6, 0.56 and 0.61, respectively) (Fig. S2b-d).

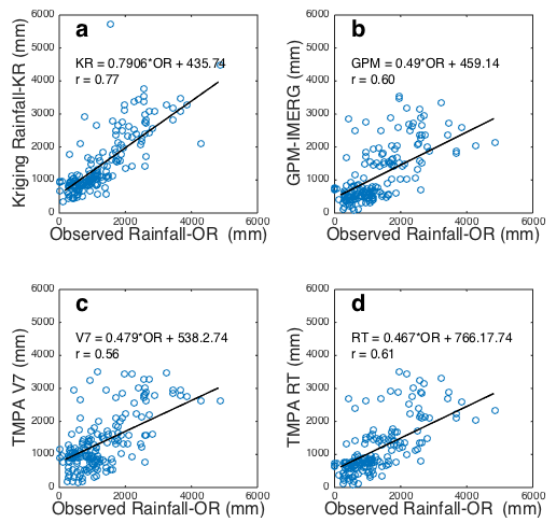


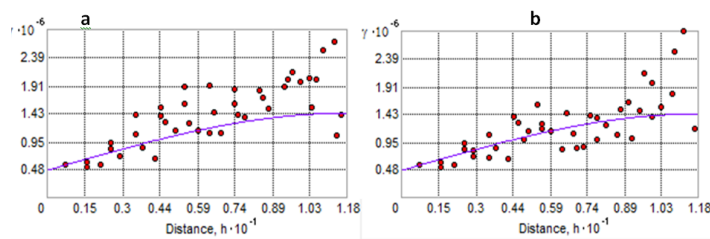
Fig.S2. Regression line between the observed annual rainfall in 181 rainfall stations (OR) and annual rainfall obtained from a) interpolation (PLU), b) GPM-IMERG, c) TMPA V7, d) TMPA RT for the 2014-2015 period.

Espinoza, J.C, Ronchail, J., Guyot, J.L., Cochonneau, G., Filizola, N.P., Lavado, C., De Oliveira, E., Pombosa, R., Vauchel P.: Spatio-Temporal rainfall variability in the Amazon basin countries (Brazil, Peru, Bolivia, Colombia and Ecuador), *I.J. of Climatology* 29(11): 1574–1594, doi:10.1002/joc.1791, 2009.

Laraque, A., Ronchail, J., Cochonneau, G., Pombosa, R., Guyot, J.L.: Heterogeneous distribution of rainfall and discharge regimes in the Ecuadorian Amazon basin, *Journal of Hydrometeorology* 8: 1364–1381, doi:10.1175/2007JHM784.1, 2007.

2. - The authors have used kriging to provide a product at the 0.1\_ resolution over the 700000 km<sup>2</sup> basin, from a total of 181 gauges. It would be informative to know what the de-correlation distance of the variogram model is ? -Is anisotropy considered when interpolating in the montaneous areas ?

The Andean region is considered during the interpolation process. Indeed, the maximum distance of the semi-variogram selected consider both Andean and Amazonian regions (11.8° - ~1300 km). When needed, data transformations and anisotropy considerations were applied. It is important to mention, there is more uncertainty (over northern Amazonian regions and southern Andean regions) when the de-correlation distance is higher than 800 km (~0.74°) in the interpolation process (example: a and b semi-variograms, respectively).



3. - The authors provide comparison of satellite/ground product for basin average ; they should indicate what are the results when comparing only over the grid points that contain a gauge (or are within a short distance from gauges).

Thank you for your comment, first (for entire the basin), a Heidke skill score map between PLU against satellite-based precipitation were evaluated

Comparison of rainfall estimates (GPM-IMERG, TMPA RT) to PLU has been also performed using the Heidke Skill Score (HSS). HSS is based on the number of correctly predicted data where the category with the largest probability proves to be correct, as reflected in the formula:  $HSS = \frac{C-E}{N-E}$ , where C is the number of correct predictions, E is the number of correct predictions expected by chance and N is the total number of predictions. HSS = 1 refers to a perfect prediction, HSS = 0 shows no skill and HSS < 0, indicates that a prediction is worse than a random prediction.

The HSS spatial distribution estimated from daily precipitation using each satellite dataset (GPM-IMERG, TMPA V7 and TMPA RT) and PLU was calculated using thresholds (0.1, 1, 5, 10 and 20 mm/day) as a reference prediction (Fig. S3a-c). In general, for the daily scale, the HSS score varies between 0 and 0.4, indicating low skill. The mean HSS for GPM-IMERG shows a moderate HSS score of around 0.4 in the Northern region (Fig. S3a). The lowest HSS values (lower than 0.2) for GPM-IMERG are mainly located in the Andean regions, where there are more rainfall stations than in the Amazonian regions. This could be due to strong spatial variability, which is characterized by rainfall decrease with altitude and by the leeward or windward position of the stations (Espinoza et al, 2009). Low scores are also observed in more scattered areas along the ABPE when TMPA V7 and TMPA RT are analyzed (lower than 0.15). Nevertheless, this relationship is slightly improved in the northern region of the Ucayali basin (~0.2).

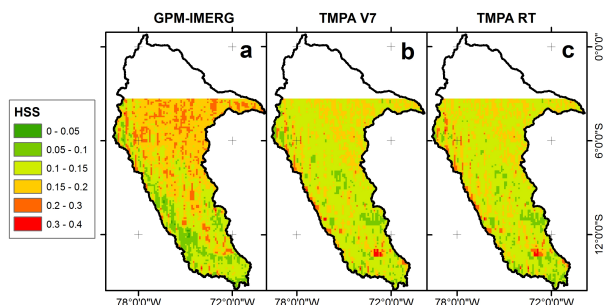


Fig. S3. Spatial variability of the Heidke Skill Score from a) GPM-IMERG, b) TMPA V7 and c) TMPA RT against PLU ground observation, period from 2014 to 2015.

Second, despite these differences, PLU and observed average rainfall show similar behavior at similar altitudes (Fig. S1). Indeed, the observed average rainfall for 181 stations shows high correlation with PLU for the 2014-2015 period ( $r = 0.77$   $p < 0.01$ ) (Fig. S2a). In contrast, observed average rainfall shows lower correlation with GPM-IMERG, TMPA V7 and TMPA RT (0.6, 0.56 and 0.61, respectively) (Fig. S2b-d).

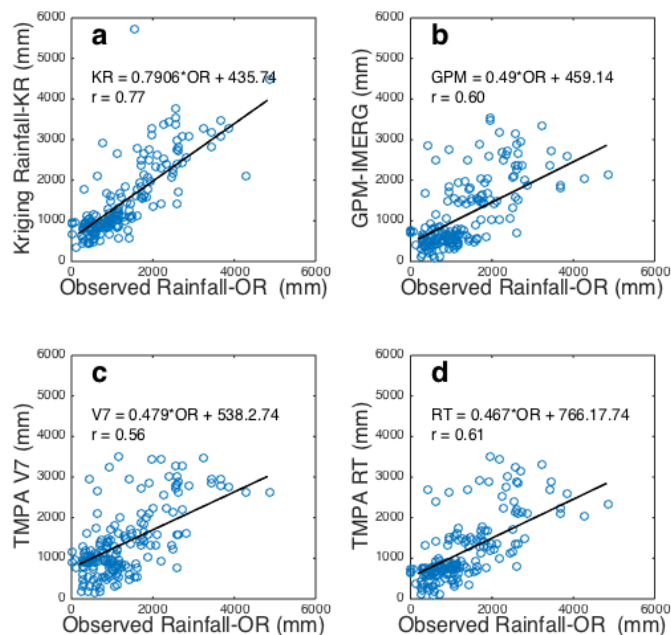


Fig.S2. Regression line between the observed annual rainfall in 181 rainfall stations (OR) and annual rainfall obtained from a) interpolation (PLU), b) GPM-IMERG, c) TMPA V7, d) TMPA RT for the 2014-2015 period.

4. - Given the points above, how certain are you that satellite products are overestimating rainfall (p 5 -section 4.1) rather than the ground based product underestimating it.

We assume that PLU is the interpolated key information (kriging) from rain gauge, which is compared to other satellites (GPM-IMERG, TMPA V7 and TMPA RT). The error of the kriging interpolation can be represented for a rainfall station as the value of the point minus the predicted value, i.e. the value on the linear regression, each point on the sub-panel Fig. S2a corresponds to a rainfall station. It is possible observing deficiencies in the KRIGING estimation, this is the case in regions with annual precipitation less than 1650 mm / year (box "a", predominant underestimation) and regions with precipitation greater than 1650 mm / year (box "b", predominant overestimation). However, rainfall obtained from Kriging interpolation method provides a better similitude with observed rainfall. ( $r = 0.77$   $p < 0.01$ ) (Fig. S2a) than other products.

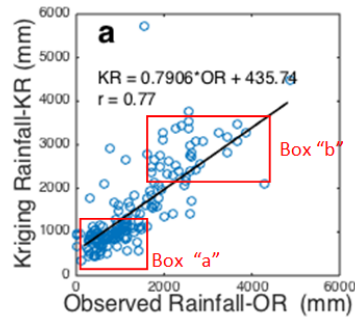


Fig.S2a. Regression line between the observed annual rainfall in 181 rainfall stations (OR) and annual rainfall obtained from a) interpolation (PLU)

5. – information on model calibration and sources of uncertainty in the model run.  
Section 4.2 :

- A description of the model configuration is lacking – the size of the HRU – and a discussion on whether or not it allows to take advantage of the products improved spatial resolution is missing.

A HRU (hydrological response unit) [Kouwen et al., 1993] approach is used to perform soil water balance by mean spatial classification of all areas with a similar combination of soil and land cover. The benefit of using HRUs is the increased accuracy in streamflow simulations at smaller scales, as they make it possible to take better advantage of high spatial resolution databases for hydrological modeling applications. To create HRUs, the watershed is divided into regular elements (cells), which are interconnected by channels. A parameter set is calculated separately for each HRU of each pixel, considering only one layer of soil [Collischonn et al., 2007]. To reduce computational time, HRUs for small areas of the ABPE surface have been merged into those composing more representative areas. Finally, The ABPE was discretized for six HRUs into 2709 by 4533 pixels (400 m spatial resolution), it allows to take advantage of the products improved like GPM-IMERG (0.1° - ~11 km spatial resolution)

Kouwen, N. & Mousavi, S. F.: WATFLOOD/SPL9: Hydrological model and flood forecasting system. In: Mathematical Models of Large Watershed Hydrology (ed. by V. P. Singh & D. K. Frevert), Water Resources Publications, Highlands Ranch, Colorado, USA, 2002.

Collischonn, W., Allasia, D.G., Silva, B.C., Tucci, C.E.M. : The MGB-IPH model for large-scale rainfall-runoff modeling, J. Hydrol. Sci. 52, 878–895, doi: 10.1623/hysj.52.5.878, 2007.

6.- How was the model calibrated and on which period/data sets ? is the model recalibrated for each rainfall forcing ? if not/yes, why ?

Ok these paragraph and Tables would be considered

To optimize the simulation of streamflows from precipitation datasets, different parameter sets were assigned to each basin in the ABPE during calibration. Analysis by sub-basin is more reliable than assigning the same

parameter set to the entire basin [Zubieta et al., 2015]. Based on sensitivity analysis of the MGB-IPH model [Collischonn et al., 2007], six parameters were selected for calibration:  $Wm_i$  (mm),  $b_i$  (-),  $Kint$  (mm.d<sup>-1</sup>),  $Kbas_i$  (mm.d<sup>-1</sup>),  $CS_i$  (-) and  $CI_i$  (-), where  $Wm$  represents water retained in the soil, which influences the evaporation process over time;  $Kint$  and  $Kbas$  control the amount of water in cases in which subsurface soil and groundwater, respectively, are saturated; and  $CS$  and  $CI$  allow for adjustment of retention time of flows [Collischonn et al., 2007]. To determine optimal parameters, an automatic calibration process was used in order to reduce the domain extent; a previous manual adjustment of the values was performed. To ensure impartiality, parameter sets were calibrated separately for each precipitation dataset. Different domains were considered initially for each parameter value, and a first value, determined by manual calibration, was defined as the relative centroid for each domain. The MOCOM-UA multi-criteria global optimization algorithm [Yapo et al., 1998] was then used to find optimal solutions for six parameters. This process results in an effective and efficient search on the Pareto optimum space [Boyle et al., 2000]. To analyze the impacts on the calibrated parameters, average parameters were calculated for precipitation datasets and HRU (Table 4).

The results of the calibration process indicate that overestimation by TMPA RT compared to observed rainfall (PLU), GPM-IMERG and TMPA V7 (Fig. 2a) in several months is consistent with a mean increase in  $Wm$  (+53%, +6%, +15% respectively), along with a predominantly mean decrease in  $Kbas$  (-18%, -39% and -16% respectively) and  $Kint$  (-25%, -15%, +2%) to achieve water balance (Table 4). Meanwhile, the overestimation by PLU compared to GPM-IMERG, TMPA V7 and TMPA RT (Fig. 3a) is consistent with a mean increase in  $Wm$  (+33%, +38%, +34% respectively), along with a mean decrease in  $Kbas$  (-30%, -28% and -38% respectively) and  $Kint$  (-17%, -16%, -17%) to achieve water balance (Table 4).

Table 3. Model parameters subjected to the process of automatic calibration for the Peruvian and Ecuadorian Amazon basin.

Parameter	HRU	Hydrological process	First guess	Domain
Wm(mm)	Shrubs, agricultural areas/not deep soils	Water storage on the HRU	200	50-1200
	Shrubs, agricultural areas/deep soils		400	50-1200
	Forest/not deep soils		350	50-1200
	Forest/deep soils		600	50-1200
	Pasture/not deep soils		120	50-1200
	Pasture/deep soils		240	50-1200
Kint(mm/d)	Shrubs, agricultural areas/not deep soils	Sub - surface flow	80	50-150
	Shrubs, agricultural areas/deep soils		90	50-150
	Forest/not deep soils		100	50-150
	Forest/deep soils		120	50-150
	Pasture/not deep soils		70	50-150
	Pasture/deep soils		80	50-150
Kbas(mm/d)	Shrubs, agricultural areas/not deep soils	Groundwater flow	30	10 - 100
	Shrubs, agricultural areas/deep soils		50	10 - 100
	Forest/not deep soils		70	10 - 100
	Forest/deep soils		80	10 - 100
	Pasture/not deep soils		55	10 - 100
	Pasture/deep soils		70	10 - 100
CS	All	Surface flow	15	0.35 - 40
CI(-)	All	Sub-surface flow	120	1 - 200
b(-)	All	Variable infiltration curve	0.12	0.01 - 2

Table 4. Values of the model mean parameters used in the *Ucayali and Huallaga basins for each rainfall datasets for the 2014-2015 period.*

Parameter	HRU	UCAYALI BASIN				HUALLAGA BASIN			
		PLU	GPM-IMERG	TMPA V7	TMPA RT	PLU	GPM-IMERG	TMPA V7	TMPA RT
Wm(mm)	Shrubs, agricultural areas/not deep soils	268	351	294	373	100	60	65	60
	Shrubs, agricultural areas/deep soils	340	472	503	597	132	102	96	99
	Forest/not deep soils	300	408	273	344	130	101	99	96
	Forest/deep soils	422	453	445	435	250	203	180	209
	Pasture/not deep soils	144	350	261	321	101	60	66	59
Kint (mm/d)	Pasture/deep soils	196	400	454	496	150	120	116	121
	Shrubs, agricultural areas/not deep soils	141	216	151	151	190	161	163	152
	Shrubs, agricultural areas/deep soils	180	236	156	163	220	189	195	198
	Forest/not deep soils	198	123	107	108	103	162	155	160
	Forest/deep soils	200	134	108	113	120	208	199	220
Kbas (mm/d)	Pasture/not deep soils	150	110	119	122	121	160	151	150
	Pasture/deep soils	180	113	126	128	132	193	201	190
	Shrubs, agricultural areas/not deep soils	103	121	89	93	55	70	72	80
	Shrubs, agricultural areas/deep soils	113	123	100	103	61	90	94	100
	Forest/not deep soils	53	134	59	53	44	70	69	80
CS	Forest/deep soils	62	25	69	62	63	90	88	100
	Pasture/not deep soils	64	112	66	64	46	70	76	80
	Pasture/deep soils	74	113	71	71	63	90	66	100
CI(-)	All	18	16	17	17	2.6	2.4	2.6	2.5
b(-)	All	112	111	118	111	111	133	135	132
		0.13	0.17	0.15	0.12	0.12	0.15	0.14	0.14

Yapo, P.O., Gupta, H.V., Sorooshian, S.: Multi-objective global optimization for hydrologic models. *Journal of Hydrology* 204, 83–97, 1998.

Boyle, D.P., Gupta, H.V., Sorooshian, S.: Toward improved calibration of hydrologic models: combining the strengths of manual and automatic methods. *Water Resources Research* 36 (12), 3663–3674, 2000.

Collischonn, W., Allasia, D.G., Silva, B.C., Tucci, C.E.M.: The MGB-IPH model for large-scale rainfall-runoff modeling. *J. Hydrol. Sci.* 52, 878–895, doi: 10.1623/hysj.52.5.878, 2007.

Zubieta, R., Geritana, A., Espinoza, J.C. and Lavado W.: Impacts of Satellite-based Precipitation Datasets on Rainfall-Runoff Modeling of the Western Amazon Basin of Peru and Ecuador, *Journal of Hydrology*, doi:10.1016/j.jhydrol.2015.06.064, 2015.

7. - One of the benefit expected from new rainfall product like i-merg is their improved space/time resolution compared to coarser products. This important point is not discussed in the study. As the model is run a daily time step the benefit of improved time resolution cannot be assessed, however the authors could investigate the impact of the 0.1\_ grid provided by i-merg. For instance by smoothing or under sampling the product to a coarser resolution (0\_5 for instance). And comparing the simulated discharge for both 0\_1 and a coarser spatial resolution.

To analyze the new benefits using GPM-IMERG in the hydrological modeling (*0.1-degree by 0.1-degree spatial resolution*, while TMPA has *0.25°\*0.25° spatial resolution*) both small (< 20,000 Km<sup>2</sup>) and large (> 20,000 km<sup>2</sup>) basins were modeled. For example: Drainage areas (< 20,000 Km<sup>2</sup>) controlled at Mejorada and KM105 stations using GPM-IMERG in the hydrological modeling are approximately evaluated from 134 and 77 pixels, respectively. Meanwhile, TMPA only approximately provides 24 and 16 pixels respectively.

Our results indicate that hydrological modeling are better using GPM-IMERG (NS=0.90) than TMPA V7 and TMPA RT (NS = 0.80 and 0.68, respectively) in drainage area controlled at KM105 station. However, results are more similar between them (NS ~0.65) in drainage area controlled at Mejorada station. It is important to note, that results of hydrological modeling using satellite-based precipitation datasets are better when small basins are assessed in Ucayali basin.

It is important to note that the advantages of GPM-IMERG over TMPA-V7 for estimating streamflows, such as temporal resolution (30 minutes compared to 3 hours, respectively), have not yet been fully analyzed. The use of sub-daily rainfall data can be potentially useful for simulating discharge in the Andean rivers, where short convective rainfall episodes are more relevant for hydrological variability. In this study, precipitation and streamflows were analyzed at a daily time step. Further flash flood modeling at smaller scales would reveal the effects of sub-diurnal differences between datasets.

8. - Rainfall is not the only source of uncertainty in the simulated discharge ; the ability of the chosen model to represent the hydrological processes in the studied region, especially in the mountainous sub-basins, should be discussed. Other sources of uncertainty—among them model parameters estimation- that might impact the results should also be mentioned and if they have been quantified, the information should be provided.

Thank you so much, this comment has been added in the manuscript

It is important to note that advantages of GPM-IMERG compared to the TMPA-V7, such as the temporal resolution (30 minutes against 3 hours, respectively), for estimating streamflows have not yet been fully analyzed. The use of sub-daily rainfall data is potentially interesting to simulate discharge variability in the Andean rivers, where short convective rainfall episodes are more relevant for hydrological variability. In this study, precipitation and streamflows were analyzed at the daily time step. Further flash flood modeling at smaller scales would be able to evidence the effects of sub-diurnal differences between datasets. Errors in streamflow simulations are mostly associated to input data uncertainty, including rainfall, limited representations of physical processes in models, and parameters such as DEM and HRUs. However, results show that it is possible to employ remote sensing data to large-scale hydrological models for streamflow simulations.

9. - importantly I could not find the information on the version of i-merg which has been used here.

GPM (product final IMERG-V03D was considered),

10. - Since there were several releases of i-merg since the launch and given that i-merg (just like 3B42) is provided with a gauge calibrated version and an un-calibrated or RT version, both should be tested here. For a fair comparison with 3B42 RT and v7.

GPM-IMERG provides data :

- The Day-1 IMERG Final Run data sets (for the GPM era, mid-March 2014 to the present, delayed about 3 months) were released in late December 2014.
- The IMERG Late Run data sets begin 7 March 2015, while the Early Run start 1 April 2015.

We tried to expand the analysis period (more than June 2015), nonetheless, we had some disadvantages with data availability of this study (streamflow and rainfall gauges) to evaluate for example Early and Late Run products (to include calibration and validation period). We are sorry.

11. - P3 – line 15 to 35 – The degree of information on products should be the same for both i-merg and 3B42 : number /type of contribution satellites, basic description of the stimulation method.

GPM is an international US/Japanese Earth science mission involving NASA and JAXA, respectively. The GPM mission improved and expanded on TRMM. GPM and TRMM provide precipitation data derived from different passive microwave (PMW) sources used in IMERG and TMPA, respectively [Huffman et al. 2015], including: Sounder for Atmospheric Profiling of Humidity in the Intertropics by Radiometry (SAPHIR), Advanced Technology Microwave Sounder (ATMS), Atmospheric Infrared Sounder (AIRS), Cross-Track Infrared Sounder (CRIS), and TRMM Combined Instrument (TCI) algorithms (2B31). They also include TRMM Microwave Imager (TMI, data ended on 8 Apr 2015), GPM Microwave Imager (GMI), Advanced Microwave Scanning Radiometer for Earth Observing Systems (AMSR-E), Special Sensor Microwave Imager/Sounder (SSMIS), Microwave Humidity Sounder (MHS), Special Sensor Microwave Imager (SSM/I), Advanced Microwave Sounding Unit (AMSU), Operational Vertical Sounder (TOVS) and microwave-adjusted merged geo-infrared (IR). The precipitation datasets used in this study are as follows:

- a) GPM (product IMERG-V03D) data at several levels of processing have been provided since March 2014 (GPM-IMERG data are available at <http://pmm.nasa.gov/GPM>). The input precipitation estimates are computed using raw satellite measurements, such as those from passive microwave sensors (TMI, AMSR-E, SSM/I, SSMIS, AMSU, MHS, SAPHIR, GMI, ATMS, TOVS, CRIS and AIRS), inter-calibrated to the GPM Combined Instrument (GCI, using GMI and Dual-frequency Precipitation Radar, DPR) and adjusted with monthly surface precipitation gauge analysis data (where available). All these datasets are used to obtain the best estimate of global precipitation maps. The temporal resolution of IMERG-V03D is *half-hourly*, and it has a 0.1-degree by 0.1-degree spatial resolution. Unlike other satellites, such as TRMM, GPM-IMERG can detect both light and heavy rain and snowfall.
- b) TMPA 3B42 version 7 is obtained from the preprocessing of data provided by different satellite-based sensors between 1998 and April 2015, in both real and near-real time (TMPA 3b42 data are available at <ftp://disc2.nascom.nasa.gov/data/TRMM/Gridded/3B42RT>). The 3B42 algorithm (every three hours) combines precipitation estimates from TMI, AMSR, SSMIS, SSM/I, AMSU, MHS, TCI, *MetOp-B* and IR. After the preprocessing is complete, the 3-hourly multi-satellite estimations are summed for the month and combined with monthly rainfall obtained from Global Precipitation Climatology Centre (GPCC), which uses ground-based precipitation. The last step is to scale each 3-hourly rainfall estimate for the month to sum to the monthly value (for each pixel separately, 0.25-degree by 0.25-degree spatial resolution).

- c) TMPA RT (real time) precipitation data are related to TMPA V7, but do not include calibration measurements of rainy seasons, which are incorporated more than a month after the satellite data. (<ftp://disc2.nascom.nasa.gov/data/TRMM/Gridded/3B42RT>). As with TMPA V7, the final, gridded, sub-daily temporal resolution of TMPA RT is usually every three hours, with a 0.25-degree by 0.25-degree spatial resolution.
- d) To evaluate satellite-based datasets, a precipitation product was obtained using daily data series (PLU) from SENAMHI rainfall stations. We collected daily rainfall data for 202 rain stations during the selected period. Quality control based on the Regional Vector Method (RVM) was used to select stations having the lowest probability of errors in their data series [Hiez 1977; Brunet-Moret 1979]. Finally, 181 RVM-approved rainfall data series [distributed over 700,000 km<sup>2</sup>] were selected, with data between March 2014 and June 2015 (Fig. 1b). The area with the highest data availability covers around 81% of the ABPE (19% without availability is mainly located in the northern region), where the largest distribution of rainfall stations is in the Andean regions, rather than Amazonian regions, of the Ucayali and Huallaga basins (the Huallaga is a sub-basin of the Marañón basin). For comparison, both regions with and without availability of rainfall data were considered for hydrological modeling. Rainfall observations subsequently were spatially interpolated to a resolution of 0.1° × 0.1° by ordinary kriging, and a spherical semivariogram model was used to generate a gridded daily rainfall dataset. Data transformations and anisotropy were applied when necessary. This method has been used to interpolate environmental variables, such as rainfall in the Amazon and Andean regions (Guimberteau et al., 2012; Zubieta et al., 2016). To use each precipitation dataset as input to the hydrological model, sub-daily data (for example, TMPA datasets have temporal resolution of 3 hours) were rescaled to a daily time step.

Guimberteau, M., Drapeau, G., Ronchail, J., Sultan, B., Polcher, J., Martinez, J.M., Prigent, C., Guyot, J.L., Cochonneau, G., Espinoza, J.C., Filizola, N., Fraizy, P., Lavado, W., De Oliveira, E., Pombosa, R., Noriega, L., Vauchel, P.: Discharge simulation in the sub-basins of the Amazon using ORCHIDEE forced by new datasets. *Hydrol. Earth Syst. Sci.* 16, 911–935, 2012.

Huffman, G.J., Bolvin, D.T., Nelkin, E.J.: Day 1 IMERG Final Run Release Notes; NASA Goddard Earth Sciences Data and Information Services Center: Greenbelt, MD, USA, 2015.

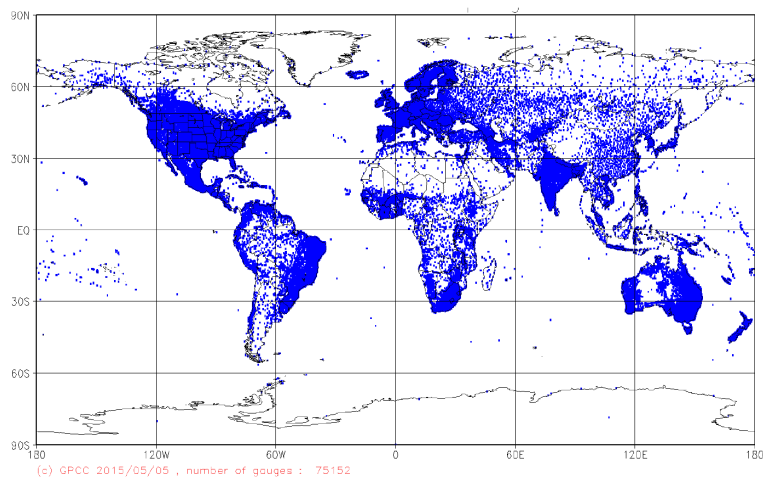
Zubieta, R., Saavedra, M., Silva, Y., Giraldez, L.: Spatial analysis and temporal trends of daily precipitation concentration in the Mantaro River basin - Central Andes of Peru. *Stochastic Environmental Research and Risk Assessment*. DOI :10.1007/s00477-016-1235-5, 2016.

Brunet-Moret, Y.: Homogénéisation des précipitations. *Cahiers ORSTOM, Série Hydrologie* 16: 3–4, 1979.

Hiez, G.: L'homogénéité des données pluviométriques, *Cahier ORSTOM, série Hydrologie* 14: 129–172, 1977. Huffman, G., Adler, R., Bolvin, D., Gu, G., Nelkin, E., Bowman, K., Hong, Y., Stocker, E., Wolff, D.: The TRMM Multisatellite Precipitation Analysis (TCMA): quasi-global, multiyear, combined-sensor precipitation estimates at fine scales, *Journal of Hydrometeorology* 8, 38–55, doi:10.11.532.5634, 2007.

12. - 3B42 (and i-merg calibrated version) use some gauges from weather services – Could you check which are the gauges used here were included in TMPA/i-merg correction stage ?

Both TMPA and GPM-IMERG adopt the Global Precipitation Climatology Centre (GPCC) monthly rain gauge analysis (Huffman et al. 2015). The Monitoring Product is represented on internationally exchanged meteorological data i.e. gauge observations from world-wide 6,000 to 7,000 stations (see next figure, (Schneider et al., 2015). The average gauge density is about 2 gauges per 2.5° by 2.5° lat/long grid box only. Building upon the figure of rainfall stations and lat/long grid (Schneider et al., 2014), it very probably that 105 rainfall stations used in our study were considered by GPCC calculations.



*Spatial distribution of monthly in-situ stations with a climatological precipitation normal, based on at least 10 years of data in GPCP data base (Schneider et al., 2014).*

Huffman, G.J., Bolvin, D.T., Nelkin, E.J.: Day 1 IMERG Final Run Release Notes; NASA Goddard Earth Sciences Data and Information Services Center: Greenbelt, MD, USA, 2015.

Schneider, U., Becker, A., Finger, P. et al. GPCP's new land surface precipitation climatology based on quality-controlled in situ data and its role in quantifying the global water cycle. *Theor Appl Climatol* (2014) 115: 15. doi:10.1007/s00704-013-0860-x

Other minor corrections :

13. -In the introduction and throughout the text there seem to be some confusion between i) the satellite themselves (TRMM or GPM core satellite)

Thanks, this paragraph would be improved as well:

The aim of this paper is to evaluate the use of rainfall estimates from the GPM-IMERG in obtaining streamflows over the Amazon Basin of Peru and Ecuador (ABPE) during a 16-month period (from March 2014 to June 2015) when all datasets are available. It provides a comparative analysis of the GPM-IMERG, TMPA RT and TMPA V7 datasets with ground-based precipitation dataset (PLU). PLU was developed by spatial interpolation using the Peruvian National Meteorology and Hydrology Service (SENAMHI) network. *Each precipitation dataset was used as input for the MGB-IPH hydrological model [Collischonn et al., 2007], which was recently adapted to ABPE [Zubieta et al., 2015].*

Zubieta, R., Geritana, A., Espinoza, J.C. and Lavado W.: Impacts of Satellite-based Precipitation Datasets on Rainfall-Runoff Modeling of the Western Amazon Basin of Peru and Ecuador, *Journal of Hydrology*, doi:10.1016/j.jhydrol.2015.06.064, 2015.

Collischonn, W., Allasia, D.G., Silva, B.C., Tucci, C.E.M. : The MGB-IPH model for large-scale rainfall-runoff modeling, *J. Hydrol. Sci.* 52, 878–895, doi: 10.1623/hysj.52.5.878, 2007.

14. ii) satellite constellations (the GPM international program includes the NASA-JAXA GPM core satellite - and TRMM while it was still going- and a constellation of other satellites from various agencies)

Thank you, this comment was considered

GPM is an international US/Japanese Earth science mission with the agencies of NASA and JAXA, respectively. GPM is an improved and expanded mission to TRMM. GPM and TRMM provide precipitation data derived from passive microwave (PMW) sources used in IMERG and TMPA, respectively [Huffman et al. 2015] .....

Huffman, G., Adler, R., Bolvin, D., Gu, G., Nelkin, E., Bowman, K., Hong, Y., Stocker, E., Wolff, D.: The TRMM Multisatellite Precipitation Analysis (TCMA): quasi-global, multiyear, combined- sensor precipitation estimates at fine scales, Journal of Hydrometeorology 8, 38–55, doi:10.1175/1525-5634(2007)08<0038:TCMA>2.0.CO;2

15. iii) the rainfall products which are derived from this satellite constellations and do not depend on one particular satellite (TMPA 3B42 can be run without the TRMM satellite itself : : i-merg could be run without GPMcore if necessary ) . Example : intro p2 line 12-13 : 'satellite data sets : : ...are uniformly distributed in space and time' - Product like 3B42 or i-merg are provided on a regular space-time grid however the microwave satellite information itself is provided with a very irregular sampling and depends on individual orbits : : . And as for gauges interpolation is done to provide a final regularly gridded product.

I am sorry, you are right, the comment would be improved

Satellite-based datasets uniformly distributed in both space and time offer an alternative for modeling hydrological events

16. P 2 – line 30-32 – confusion between GPMcore single satellite launched in 2014, and the GPM multi satellite/multiagencies constellation : : :..

Also : The improved resolution capacity of the latest products does not come from a specific satellite (though some members of the GPM constellation such as TRMM and more recently Megha-Tropiques , provide additional sampling specifically in the Tropics) but from the overall sampling capacity of the whole constellation. This should be mentioned more clearly in the intro.

Thank you, this paragraph would be included

The GPM mission [Schwallier and Morris, 2011], launched in February 2014, comprises an international constellation of satellites that provide rainfall estimations with significant improvements in spatio-temporal resolution, compared to TMPA products. This is true of GPM products such as Integrated Multi-satellite Retrievals (IMERG) estimations. Recent studies highlight that the GPM-IMERG estimations can adequately substitute for TMPA estimations both hydrologically and statistically, despite limited data availability [Liu, 2016; Tang et al., 2016].

Schwallier, M. R. and K. R. Morris.: A Ground Validation Network for the Global Precipitation Measurement Mission, J. Atmos. Oceanic Technol., 28, 301–319, doi: 10.1175/2010jtecha1403.1. 2011.

Liu, Z.: Comparison of Integrated Multisatellite Retrievals for GPM (IMERG) and TRMM Multisatellite Precipitation Analysis (TMPA) monthly precipitation products: Initial results, J. Hydrometeor., 17, 777–790, doi:10.1175/JHM-D-15-0068.1, 2016.

Tang, G., Z. Zeng, D. Long, X. Guo, B. Yong, W. Zhang, and Y. Hong.: Statistical and hydrological comparisons between TRMM and GPM level-3 products over a midlatitude basin: Is day-1 IMERG a good successor for TMPA 3B42V7?, J. Hydrometeor., 17, 121–137, doi:10.1175/jhm-d-15-0059.1, 2016.

**MANUSCRIPT WITH INSERTIONS AND  
CHANGES**

# Hydrological modeling of the Peruvian-Ecuadorian Amazon basin using GPM-IMERG satellite-based precipitation dataset

Ricardo Zubieta<sup>1,2</sup>, Augusto Getirana<sup>3,4</sup>, Jhan Carlo Espinoza<sup>1,2</sup>, Waldo Lavado-Casimiro<sup>5,2</sup>, Luis Aragon<sup>2</sup>

<sup>1</sup> Subdirección de Ciencias de la Atmósfera e Hidrosfera (SCAH), Instituto Geofísico del Perú (IGP), Lima, Peru

<sup>2</sup> Programa de Doctorado en Recursos Hídricos, Universidad Nacional Agraria La Molina, Peru

<sup>3</sup> Hydrological Sciences Laboratory, NASA Goddard Space Flight Center, Greenbelt, MD, USA

<sup>4</sup> Earth System Science Interdisciplinary Center, College Park, MD, USA

<sup>5</sup> Servicio Nacional de Meteorología e Hidrología (SENAMHI), Lima, Peru

Correspondence to: R. Zubieta (ricardo.zubieta@igp.gob.pe).

## Abstract

In the last two decades, rainfall estimates provided by the Tropical Rainfall Measurement Mission (TRMM) have proven applicable in hydrological studies. The Global Precipitation Measurement (GPM) mission, which provides the new generation of rainfall estimates, is now considered a global successor to TRMM. The usefulness of GPM data in hydrological applications, however, has not yet been evaluated over the Andean and Amazonian regions. This study uses GPM data provided by the Integrated Multi-satellite Retrievals (IMERG) (product/final run) as input to a distributed hydrological model for the Amazon Basin of Peru and Ecuador for a 16-month period (from March 2014 to June 2015) when all datasets are available. TRMM products (TMPA V7, TMPA RT datasets) and a gridded precipitation dataset processed from observed rainfall are used for comparison. The results indicate that precipitation data derived from GPM-IMERG correspond more closely to TMPA V7 than TMPA RT datasets, but both GPM-IMERG and TMPA V7 precipitation data tend to overestimate, compared to observed rainfall (by 11.1% and 15.7 %, respectively). In general, GPM-IMERG, TMPA V7 and TMPA RT

Con formato: Color de fuente: Texto 1

Con formato: Sangría: Izquierda: 0 cm, Sangría francesa: 1.27 cm

Con formato: Sangría: Izquierda: 0 cm, Sangría francesa: 1.27 cm

Con formato: Color de fuente: Texto 1, español

Con formato: Color de fuente: Texto 1

Con formato: Color de fuente: Texto 1, español

Con formato: Color de fuente: Texto 1

Con formato: Color de fuente: Texto 1, Inglés (americano)

Con formato: Color de fuente: Texto 1

Con formato: Color de fuente: Texto 1, Inglés (americano)

Con formato: Color de fuente: Texto 1

Con formato: Sangría: Izquierda: 0 cm, Sangría francesa: 1.27 cm

Con formato: Color de fuente: Texto 1, Inglés (americano)

Con formato: Color de fuente: Texto 1

Con formato: Color de fuente: Texto 1, Inglés (americano)

Con formato: Color de fuente: Texto 1

Con formato: Color de fuente: Texto 1

Eliminado: in comparison

Con formato: Color de fuente: Texto 1

correlate with observed rainfall, with a similar number of rain events correctly detected (~20%). Statistical analysis of modeled streamflows indicates that GPM-IMERG is as useful as TMPA V7 or TMPA RT datasets in southern regions (Ucayali basin). GPM-IMERG, TMPA V7 and TMPA RT do not properly simulate streamflows in northern regions (Marañón and Napo basins), probably because of the lack of adequate rainfall estimates in northern Peru and the Ecuadorian Amazon.

Keywords: GPM; Precipitation datasets; Hydrological modeling; Amazon/Andes; TRMM

## 1. Introduction

Satellite-based precipitation data have been widely used for hydrometeorological applications, such as hydrological modeling, especially in data-sparse regions like the Amazon River basin [Collischonn et al, 2008; Getirana et al, 2011; Paiva et al., 2013, Zulkafli et al., 2014; Zubieta et al., 2015]. Rainfall is extremely variable in both space and time, particularly over regions characterized by topographic contrast, such as the western Amazon Basin [Espinoza et al., 2009; Lavado et al., 2012]. In this region, the Andes Mountains contribute to high spatio-temporal variability of rainfall [Laraque et al., 2007, Espinoza et al., 2015]. To improve approximation and reduce uncertainty, detailed monitoring is needed using a high-density rain gauge network. Only a low-density rain gauge network is available in the Amazon basin (AB), however, which limits understanding of hydrological processes and hydrological modeling over the region [Getirana et al., 2011; Paiva et al., 2013]. Satellite-based datasets, uniformly distributed in both space and time, offer an alternative for modeling hydrological events. Their usefulness in Andean-Amazon basins and their applicability as input to hydrological models have been evaluated recently by comparing modeled and observed datasets. Results indicate that these datasets could be used for operational applications in some Andean-Amazon regions [Zulkafli et al., 2014; Zubieta et al., 2015]. However, hydrological modeling using satellite-based precipitation data does not yield successful results in equatorial regions. This is mainly because of inadequate satellite estimates, because streamflows resulting from hydrological modeling using observed rainfall show acceptable performance in the Napo River basin in the equatorial region [Zubieta et al., 2015].

**Con formato:** Fuente de párrafo predeter.,Color de fuente: Texto 1, español

**Con formato:** Color de fuente: Texto 1

**Eliminado:** , because they are uniformly distributed in both space and time.

**Con formato:** hps,Fuente:11 pt, Color de fuente: Texto 1, español

**Con formato:** Color de fuente: Texto 1

**Con formato:** Color de fuente: Texto 1

**Eliminado:** This could improve streamflow

**Con formato:** Fuente de párrafo predeter.,Color de fuente: Texto 1, español

**Eliminado:** and relationships between model parameters in unmonitored basins.

**Movido (inserción) [1]**

**Con formato:** Color de fuente: Texto 1

**Con formato:** Fuente:NimbusSanL-Regu, Color de fuente: Texto 1

Hydrological modeling and forecasting are still poorly developed in the Andean and Amazonian regions. It is important to improve these tools, especially because of an intensification of extreme hydrological events in the Amazon basin [Gloor et al., 2013], such as intense droughts in 2005 and 2010 [Marengo et al., 2008; Marengo et al., 2011; Espinoza et al., 2011] and severe floods in 2009, 2012 and 2014 [Espinoza et al., 2012; 2013; 2014]. Moreover, a high percentage of total annual precipitation can fall in just a few days, causing soil erosion and landslides [Zubieta et al., 2016]

In the last two decades, advances in satellite technology have improved rainfall estimation in much of the world [Huffman et al., 2007]. The Tropical Rainfall Measuring Mission (TRMM) Multi-satellite Precipitation Analysis (TMPA) precipitation dataset [Huffman et al., 2007] has been important for research and for many hydrological applications in Amazon regions, and there is consensus among studies using TMPA in Amazon regions [Collischonn et al., 2008; Getirana et al., 2011; Paiva et al., 2013; Zulkafli et al., 2014; Zubieta et al., 2015]. The TRMM mission ended in April 8, 2015, however, after the spacecraft depleted its fuel reserves (<https://pmm.nasa.gov/trmm/mission-end>). Despite TRMM's demise, this is not a substantive issue for some products, such as TMPA and TMPA-RT, which are expected to run in parallel with the new Global Precipitation Measurement (GPM) satellite until mid-2017 [Huffman et al., 2015]. The GPM mission [Schwaller and Morris, 2011], launched in February 2014, comprises an international constellation of satellites that provide rainfall estimations with significant improvements in spatio-temporal resolution, compared to TMPA products. This is true of GPM products such as Integrated Multi-satellite Retrievals (IMERG) estimations. Recent studies highlight that the GPM-IMERG estimations can adequately substitute for TMPA estimations both hydrologically and statistically, despite limited data availability [Liu, 2016; Tang et al., 2016].

The aim of this paper is to evaluate the use of rainfall estimates from GPM-IMERG for obtaining streamflows over the Amazon Basin of Peru and Ecuador (ABPE) during a 16-month period (from March 2014 to June 2015) for which all datasets are available. It provides a comparative analysis of the GPM-IMERG, TMPA RT and TMPA V7 datasets and a ground-based precipitation dataset (PLU). PLU was developed by spatial interpolation using the Peruvian National Meteorology and Hydrology Service (SENAMHI) network. Each precipitation dataset was used as input for the MGB-IPH hydrological model [Collischonn et al., 2007], which was recently adapted to the ABPE [Zubieta et al., 2015].

The ABPE extends from the tropical Andes to the Peruvian Amazon, with elevations ranging up to 6,300 meters above sea level, a drainage area of 878, 300 km<sup>2</sup> and a mean discharge of around ~35,500 m<sup>3</sup>/s at the Tabatinga station [Lavado et al., 2012]. The ABPE is located in the northwestern AB (Fig. 1a), and its

- Con formato ... [1]
- Eliminado: this tool ... [1]
- Con formato ... [2]
- Eliminado: , ... [2]
- Con formato ... [3]
- Eliminado: ... [3]
- Con formato ... [4]
- Eliminado: to ... [4]
- Con formato ... [5]
- Eliminado: to ... [5]
- Con formato ... [6]
- Eliminado: on ... [6]
- Con formato ... [7]
- Eliminado: (<https://pmm.nasa.gov/trmm/mission-end>). ... [7]
- Eliminado: the actual ... [7]
- Con formato ... [9]
- Eliminado: of TRMM ... [9]
- Con formato ... [10]
- Eliminado: the ... [10]
- Con formato ... [8]
- Con formato ... [11]
- Eliminado: ... [11]
- Con formato ... [12]
- Eliminado: GPM ( ... [12]
- Con formato ... [13]
- Eliminado: GPM, which was ... [13]
- Con formato ... [14]
- Eliminado: provides a new generation of ... [14]
- Con formato ... [15]
- Eliminado: estimation every three hours [Schwaller ... [16]
- Con formato ... [17]
- Eliminado: even with its ... [17]
- Con formato ... [18]
- Eliminado: ... [18]
- Con formato ... [19]
- Con formato ... [20]
- Eliminado: the ... [20]
- Con formato ... [21]
- Eliminado: in ... [21]
- Con formato ... [22]
- Eliminado: when ... [22]
- Con formato ... [23]
- Eliminado: datasets and TRMM ( ... [23]
- Con formato ... [24]
- Eliminado: products). For comparison with satellit ... [25]
- Con formato ... [26]
- Eliminado: from observed rainfall ... [26]
- Con formato ... [27]
- Eliminado: ... [27]
- Con formato ... [28]
- Eliminado: northwest of the ... [28]
- Con formato ... [29]

area corresponds to 14% of the AB. It consists mainly of basins such as the Ucayali basin (southern ABPE), Marañón basin (Western of the ABPE) and Napo basin (northern ABPE) (Fig. 1b).

## 2. Datasets used

GPM is an international US/Japanese Earth science mission involving NASA and JAXA, respectively. The GPM mission improved and expanded on TRMM. GPM and TRMM provide precipitation data derived from different passive microwave (PMW) sources used in IMERG and TMPA, respectively [Huffman et al. 2015], including: Sounder for Atmospheric Profiling of Humidity in the Intertropics by Radiometry (SAPHIR), Advanced Technology Microwave Sounder (ATMS), Atmospheric Infrared Sounder (AIRS), Cross-Track Infrared Sounder (CRIS), and TRMM Combined Instrument (TCI) algorithms (2B31). They also include TRMM Microwave Image (TMI, data ended on 8 Apr 2015), GPM Microwave Imager (GMI), Advanced Microwave Scanning Radiometer for Earth Observing Systems (AMSR-E), Special Sensor Microwave Imager/Sounder (SSMIS), Microwave Humidity Sounder (MHS), Special Sensor Microwave Imager (SSM/I), Advanced Microwave Sounding Unit (AMSU), Operational Vertical Sounder (TOVS) and microwave-adjusted merged geo-infrared (IR). The precipitation datasets used in this study are as follows:

- e) GPM (product IMERG-V03D) data at several levels of processing have been provided since March 2014 (GPM-IMERG data are available at <http://pmm.nasa.gov/GPM>). The input precipitation estimates are computed using raw satellite measurements, such as those from passive microwave sensors (TMI, AMSR-E, SSM/I, SSMIS, AMSU, MHS, SAPHIR, GMI, ATMS, TOVS, CRIS and AIRS), inter-calibrated to the GPM Combined Instrument (GCI, using GMI and Dual-frequency Precipitation Radar, DPR) and adjusted with monthly surface precipitation gauge analysis data (where available). All these datasets are used to obtain the best estimate of global precipitation maps. The temporal resolution of IMERG-V03D is half-hourly, and it has a 0.1-degree by 0.1-degree spatial resolution. Unlike other satellites, such as TRMM, GPM-IMERG can detect both light and heavy rain and snowfall.
- f) TMPA 3B42 version 7 is obtained from the preprocessing of data provided by different satellite-based sensors between 1998 and April 2015, in both real and near-real time (TMPA 3b42 data are available at <ftp://disc2.nascom.nasa.gov/data/TRMM/Gridded/3B42RT>). The 3B42 algorithm (every three hours) combines precipitation estimates from TMI, AMSR, SSMIS, SSM/I, AMSU, MHS, TCI, *MetOp-B* and IR. After the preprocessing is complete, the 3-hourly multi-satellite estimations are summed for the month and combined with monthly rainfall obtained from Global Precipitation Climatology Centre (GPCC), which uses ground-based precipitation. The last step is to scale each 3-hourly rainfall estimate for the

**Eliminado:** of the  
**Con formato:** Color de fuente: Texto 1  
**Eliminado:** Northern of the  
**Con formato:** Color de fuente: Texto 1  
**Eliminado:** in hydrological modeling  
**Con formato:** Color de fuente: Texto 1

**Eliminado:** <#>GPM and TRMM are satellite missions of the space agencies of the United States (NASA) and Japan (JAXA). They provide precipitation data derived from their products, which are evaluated in this study: .  
**Con formato:** Color de fuente: Texto 1  
**Eliminado:** <#>final  
**Con formato:** Color de fuente: Texto 1  
**Con formato:** Color de fuente: Texto 1  
**Con formato:** Color de fuente: Texto 1  
**Eliminado:** <#>),  
**Con formato:** Color de fuente: Texto 1  
**Eliminado:** <#> and making  
**Con formato:** Color de fuente: Texto 1  
**Eliminado:** <#> using combinations of observations and other meteorological data (<http://www.nasa.gov/gpm>). IMERG was designed to improve the limited sampling available from single low earth orbit (leo) satellites by using as many leo-satellites as possible, using geosynchronous-Earth-orbit (geo) infrared (IR) estimates to fill in gaps [Huffman et al.,  
**Subido [1]:** <#>2015].  
**Con formato:** Color de fuente: Texto 1  
**Eliminado:** <#>  
**Con formato:** Color de fuente: Texto 1  
**Eliminado:** <#>15  
**Con formato:** Color de fuente: Texto 1  
**Eliminado:** <#>15  
**Con formato:** Color de fuente: Texto 1  
**Con formato:** Color de fuente: Texto 1  
**Con formato:** Color de fuente: Texto 1  
**Eliminado:** a set  
**Con formato:** Color de fuente: Texto 1

[month to sum to the monthly value \(for each pixel separately, 0.25-degree by 0.25-degree spatial resolution\)](#).

g) [TMPA RT \(real time\) precipitation data are related to TMPA V7, but do not include calibration](#) measurements of rainy seasons, which are incorporated more than a month after the satellite data. (<ftp://disc2.nascom.nasa.gov/data/TRMM/Gridded/3B42RT>). As with TMPA V7, the final, gridded, sub-daily temporal resolution of TMPA RT is usually every three hours, with a 0.25-degree by 0.25-degree spatial resolution.

h) [To evaluate satellite-based datasets, a precipitation product was obtained using daily data series \(PLU\) from SENAMHI rainfall stations. We collected daily rainfall data for 202 rain stations](#) during the selected period. Quality control based on the Regional Vector Method (RVM) was used to select stations having the lowest probability of errors in their data series [Hiez 1977; Brunet-Moret 1979]. Finally, 181 RVM-approved rainfall data series [distributed over 700,000 km<sup>2</sup>] were selected, with data between March 2014 and June 2015 (Fig. 1b). The area with the highest data availability covers around 81% of the ABPE (19% without availability is mainly located in the northern region), where the largest distribution of rainfall stations is in the Andean regions, rather than Amazonian regions, of the Ucayali and Huallaga basins (the Huallaga is a sub-basin of the Marañón basin). For comparison, both regions with and without availability of rainfall data were considered for hydrological modeling. Rainfall observations subsequently were spatially interpolated to a resolution of 0.1° × 0.1° by ordinary kriging, and a spherical semivariogram model was used to generate a gridded daily rainfall dataset. [Data transformations and anisotropy were applied when necessary. This method has been used to interpolate environmental variables, such as rainfall in the Amazon and Andean regions \(Guimberteau et al., 2012; Zubieta et al., 2016\)](#). [To use each precipitation dataset as input to the hydrological model, sub-daily data \(for example, TMPA datasets have temporal resolution of 3 hours\) were rescaled to a daily time step.](#)

To evaluate model results, streamflow series from the SO-HYBAM Observatory ([www.ore-hybam.org](http://www.ore-hybam.org)) and SENAMHI stations for the selected period were used; these were KM105 (KM), Mejorada (ME), Chazuta (CHA), Borja (BO), Bellavista (BE), Lagarto (LA), Pucallpa (PU), Requena (RE), San Regis (SR), Tamshiyacu (TAM) and Tabatinga (TAB) (Fig. 1b, Table 1). To describe climate characteristics, meteorological data from NCEP-DOE Reanalysis at surface level [[Kanamitsu et al., 2002](#)] were collected, including relative humidity, wind speed, solar radiation, air temperature and atmospheric pressure. Basin topography is derived from the Shuttle Radar

**Eliminado:** TMPA has been essential for creating spatio-temporal average levels that are appropriate for user applications, with very good results in climate and hydrological studies in recent decades [Huffman et al., 2007]. The usefulness of TMPA for hydrological modeling in the Amazon basin has been evaluated, for example, in Paiva et al., 2013; Zulkafli et al., 2014; and Zubieta et al., 2015.

**Con formato:** Color de fuente: Texto 1

**Con formato:** Color de fuente: Texto 1

**Con formato:** Color de fuente: Texto 1

**Eliminado:**

**Con formato:** Color de fuente: Texto 1

**Con formato:** Color de fuente: Texto 1

**Eliminado:** (

**Con formato:** Color de fuente: Texto 1

**Eliminado:** )

**Con formato:** Color de fuente: Texto 1

Topography Mission (SRTM, version 2). Digital thematic maps correspond to vegetation and soil maps of Peru (<http://www.fao.org>) and a vegetation type map of Ecuador (<http://sociobosque.ambiente.gob.ec/>). A soil map of Ecuador (SECS-Ecuador, <http://www.secsuelo.org>) and soil and land-use maps of Colombia (IGAC-Colombia, <http://geoportal.igac.gov.co>) were also considered. GPM-IMERG, TMPA V7, TMPA RT and PLU datasets were selected for the period corresponding to observed streamflows.

Con formato: Color de fuente: Texto 1

### 3. Methodology

The MGB-IPH model [Collischonn et al., 2007] has been used to simulate the hydrological behavior of the ABPE. It consists of modules for calculating soil water budget, evapotranspiration, flow propagation within a cell, and flow routing through the drainage network. A HRU (hydrological response unit) [Kouwen et al., 1993] approach is used to perform soil water balance by mean spatial classification of all areas with a similar combination of soil and land cover. The benefit of using HRUs is the increased accuracy in streamflow simulations at smaller scales, as they make it possible to take better advantage of high spatial resolution databases for hydrological modeling applications. To create HRUs, the watershed is divided into regular elements (cells), which are interconnected by channels. A parameter set is calculated separately for each HRU of each pixel, considering only one layer of soil [Collischonn et al., 2007]. The Muskingum-Cunge method is used for routing streamflows through the river network from runoff generated for different HRUs in the cells. Streamflows are adjusted for accuracy according to the stream reach length and slope. A detailed description of the MGB-IPH model is provided in Collischonn et al. [2007].

Eliminado: , which are associated with model parameters.

Con formato: Color de fuente: Texto 1

The comparison of precipitation datasets was performed in two steps: first, an analysis of monthly averages and detected rain events at different precipitation thresholds (0.1, 1, 5, 10 and 20 mm/day) was conducted over the ABPE. The analysis was performed by computing the frequency bias index (FBI), probability of detection (POD), false alarm ratio (FAR), and equitable threat score (ETS) (see Table 2). These are calculated from a 2 x 2 contingency matrix composed of four parameters (a, b, c, d), where a is the number of observed rain events correctly detected, b is the number of observed rain events not detected, c is the number of rainfall events detected but not observed (false alarms), and d is the sum of cases in which neither observed nor detected rain events occurred. FBI allows analysis of overestimation or underestimation of rain events, POD provides information about sensitivity to not-detected and detected events, FAR is a function of false alarms, while ETS indicates the fraction of observed and/or detected rain events that were correctly detected. Comparison of rainfall estimates (GPM-IMERG, TMPA RT) to PLU has been also performed using the Heidke Skill Score (HSS). HSS is based on the number of correctly predicted data where the category with the largest probability proves to be correct, as reflected in the formula:  $= \frac{C-E}{N-E}$ , where C is the number of correct

Con formato: Color de fuente: Texto 1

Eliminado: 0

Con formato: Color de fuente: Texto 1

predictions, E is the number of correct predictions expected by chance and N is the total number of predictions. HSS = 1 refers to a perfect prediction, HSS = 0 shows no skill and HSS < 0, indicates that a prediction is worse than a random prediction.

Con formato: Color de fuente: Texto 1

Two performance coefficients were then used to evaluate the streamflow simulations: the Nash Sutcliffe (NS) coefficient, and the difference between volumes calculated and observed ( $\Delta V$ ), shown in equations 1 and 2:

$$NS = 1 - \frac{\sum_{t=1}^{nt} (Q_{obs}(t) - Q_{cal}(t))^2}{\sum_{t=1}^{nt} (Q_{obs}(t) - \bar{Q}_{obs})^2} \quad [1]$$

Con formato: Color de fuente: Texto 1, Inglés (americano)

Con formato ... [30]

$$\Delta V = \frac{\sum(Q_{obs}(t)) - \sum(Q_{cal}(t))}{\sum(Q_{obs}(t))} \quad [2]$$

Con formato ... [31]

with  $Q_{obs}$  observed and  $Q_{cal}$  modeled streamflows. The range of efficiency lies from  $-\infty$  to 1. An efficiency of 1 ( $E = 1$ ) corresponding to a perfect fit of modeled streamflow and observed data, while an efficiency of less than zero indicates that the mean value of the time series (observed) would have been a better predictor than the model. A Taylor diagram was used to provide a graphic summary of how closely a pattern (or a set of simulated streamflows) matches observed streamflows. In this diagram, the similarity among three statistical patterns is quantified according to the amplitude of their coefficient of variation (CV %), correlation coefficient and centered root-mean-square difference (RMSD %) [Taylor, 2001]. This can be used to analyze the relative ability of hydrological models to simulate the spatial pattern of mean streamflow.

Eliminado: w

Con formato: Color de fuente: Texto 1

Eliminado: ,

Con formato: Color de fuente: Texto 1

Eliminado: a

Con formato: Color de fuente: Texto 1

Eliminado: s

Con formato: Color de fuente: Texto 1

Eliminado: .

Con formato: Color de fuente: Texto 1

Eliminado: w

Con formato: Color de fuente: Texto 1

Eliminado: ,

Con formato: Color de fuente: Texto 1

Eliminado: lower

Con formato: Color de fuente: Texto 1

#### 4. Results

##### 4.1 Ground-based precipitation dataset (PLU)

To evaluate the ability of PLU to reproduce rainfall gradients in the Andes, the relationship between annual rainfall and altitude for 181 stations was compared. In this area, 100 rainfall station are located above 2000 m asl; some record in excess of 1500 mm/year, while less than 1200 mm/year is generally recorded above 3000 m asl. At lower elevations, abundant rainfall is associated with warm, moist air and the release of a large quantity of water vapor over the first eastern slope of the Andes; as a result, the amount of rainfall decreases with altitude (Laraque et al., 2007; Espinoza et al., 2009). A group of 15 observed rainfall stations located above 2000 m asl shows rainfall amount below 450 mm/year; this group cannot be adequately

represented by PLU. Despite these differences, PLU and observed average rainfall show similar behavior at similar altitudes (Fig. S1). Indeed, the observed average rainfall for 181 stations shows high correlation with PLU for the 2014-2015 period ( $r = 0.77$   $p < 0.01$ ) (Fig. S2a). In contrast, observed average rainfall shows lower correlation with GPM-IMERG, TMPA V7 and TMPA RT (0.6, 0.56 and 0.61, respectively) (Fig. S2b-d).

#### 4.2 Comparison of GPM-IMERG and other rainfall datasets

Total annual rainfall over the ABPE during the selected period, using all four precipitation products, is shown in Figs. 1c-f. The satellite-based datasets (GPM-IMERG, TMPA V7 and TMPA RT) produce overestimates compared to observation (PLU) during this period (by 11.1%, 15.7% and 27.7 %, respectively). As Figs. 1c-f show, the satellite-based products present similar spatial distributions. These products are comparable to PLU over a) the Andean regions (for this paper, the Andean and Amazon regions are considered to be above and below 1500 meters above sea level, respectively, see Fig 1b), with precipitation mainly between 500 and 1500 mm/year, and b) the northern Amazon regions (3.0°S-6.0°S), with precipitation between 2000 and 3000 mm/year. There are some spatial differences over the southern Amazon regions. This can be attributed to greater uncertainty of the PLU dataset, however, because there are fewer rainfall stations in those regions, particularly the eastern Ucayali basin (Fig 1b).

A comparison of monthly rainfall over the Ucayali and Huallaga river basins (at the Requena and Chazuta stations) with satellite-based precipitation data during the selected period is shown in Figs. 2a and 3a. In these basins, spatial distribution of rainfall stations is greater in the Andes region than the Amazon region. The TMPA V7 and GPM-IMERG datasets are very similar to each other in the Ucayali and Huallaga river basins. A monthly rainfall analysis shows that TMPA V7 and GPM-IMERG tend to underestimate dry-season rainfall in the Ucayali basin (April to September) by 10.6%, compared to the PLU dataset (Fig. 2a). Both datasets tend to slightly overestimate wet-season rainfall, by 3%, compared to the PLU dataset. This overestimation is larger than that obtained by TMPA V7 or GPM-IMERG when TMPA RT is analyzed (17.5%). The GPM-IMERG, TMPA V7 and TMPA RT datasets tend

- Eliminado: 4.1
- Con formato: Color de fuente: Texto 1
- Eliminado: is shown in Figs. 1c-f
- Con formato: Color de fuente: Texto 1
- Eliminado: .
- Con formato: Color de fuente: Texto 1
- Eliminado: overestimate observations
- Con formato: Color de fuente: Texto 1
- Eliminado: the
- Con formato: Color de fuente: Texto 1
- Eliminado: ,
- Con formato: Color de fuente: Texto 1

- Eliminado: , where the
- Con formato: Color de fuente: Texto 1
- Eliminado: ),
- Con formato: Color de fuente: Texto 1
- Con formato: Color de fuente: Texto 1
- Eliminado: Meanwhile, both
- Con formato: Color de fuente: Texto 1
- Eliminado: s
- Con formato: Color de fuente: Texto 1
- Con formato: Color de fuente: Texto 1
- Eliminado: %
- Con formato: Color de fuente: Texto 1
- Eliminado: Moreover,
- Con formato: Color de fuente: Texto 1

to underestimate dry- and wet-season rainfall in the Huallaga basin by 30.7%, 28.2% and 26.2%, respectively, compared to PLU (Fig. 3a).

Con formato: Color de fuente: Texto 1

Building on the average number of total days of rain events (456), the number of rain events correctly detected (~ 20%) is similar for each satellite precipitation dataset, compared to the PLU dataset, over the Ucayali and Huallaga basins (Figs. 2b and 3b). The average number of events correctly and not correctly detected is also consistent—that is, all precipitation datasets are clearly better at identifying low- and moderate-precipitation events (1 - 5 mm/day) than the number of high- and very low-precipitation events (higher than 5 mm/day and lower than 1 mm/day respectively) (Figs. 2b-c and 3b-c). Average FBI values obtained for all datasets indicate a low ability to detect rain events greater than 5 mm/day, producing FBI values varying mainly between 1 and 2 in the Ucayali and Huallaga basins. This differs substantially from optimal conditions (~1) (Figs. 2f and 3f). This variation is due to the high number of rain events that were not correctly detected (~80%) (Figs. 2c and 3c). In general, the satellite-based datasets' limitation in representing rainfall may be due to their strong spatial variability in the Amazon-Andes region. The AB is distinguished by complex spatial distribution of rainfall because of the interactions between topography and large-scale humidity transport [Espinoza et al., 2015]. High or extreme precipitation events can be variable in space and time, and the amount of rainfall recorded during extreme events in an Andean location may be normal in an Amazonian one.

Con formato: Color de fuente: Texto 1

Con formato: Color de fuente: Texto 1

Eliminado: capacity in the detection of

Con formato: Color de fuente: Texto 1

Eliminado:

Eliminado:

Con formato: Color de fuente: Texto 1

Eliminado:

Con formato: Color de fuente: Texto 1

Con formato: Color de fuente: Texto 1

Eliminado: that were not correctly detected (~80%) (Figs. 2c and 3c).

Con formato: Fuente de párrafo predeter.,Color de fuente: Texto 1, Alemán

Con formato: Color de fuente: Texto 1

Eliminado: ,

Con formato: Color de fuente: Texto 1

Eliminado: s

Con formato: Color de fuente: Texto 1

Con formato: Color de fuente: Texto 1

Con formato: Color de fuente: Texto 1

Eliminado: which

Con formato: Color de fuente: Texto 1

Eliminado: rate of

Con formato: Color de fuente: Texto 1

Eliminado: alarms

Con formato: Color de fuente: Texto 1

Con formato: Color de fuente: Texto 1

Average POD values for all datasets indicate a moderate probability of detection (POD less than 0.55) of rain events greater than 5 mm/day; this probability decreases to ~0.2 for other events in the Ucayali and Huallaga basins (Figs. 2g and 3g). The average number of events correctly and not correctly detected is also consistent—that is, all precipitation datasets are clearly better at identifying precipitation events of between 1 and 5 mm/day. The low probability of detection is consistent with the fraction of rain events that were correctly detected (ETS) (Figs. 2i and 3i). This is due to a high false alarm rate (FAR) of between ~0.7 and ~0.9 for rain events higher than 5 mm/day and lower than 1 mm/day for all satellite precipitation datasets in both the Ucayali and Huallaga basins (Figs. 2h and 3h).

The limited ability to represent rainfall events of more than 5 mm/day using satellite precipitation datasets (GPM-IMERG, TMPA V7, TMPA RT), compared to PLU datasets (Figs. 2g and 3g), may be due to slight overestimation (in the Ucayali basin) or high overestimation (in the Huallaga basin), identified mainly during the wet season (Figs. 2a and 3a). Events exceeding 5mm/day are more likely to occur during that period.

The HSS spatial distribution estimated from daily precipitation using each satellite dataset (GPM-IMERG, TMPA V7 and TMPA RT) and PLU was calculated using thresholds (0.1, 1, 5, 10 and 20 mm/day) as a reference prediction (Fig. S3a-c). In general, for the daily scale, the HSS score varies between 0 and 0.4, indicating low skill. The mean HSS for GPM-IMERG shows a moderate HSS score of around 0.4 in the Northern region (Fig. S3a). The lowest HSS values (lower than 0.2) for GPM-IMERG are mainly located in the Andean regions, where there are more rainfall stations than in the Amazonian regions. This could be due to strong spatial variability, which is characterized by rainfall decrease with altitude and by the leeward or windward position of the stations (Espinoza et al, 2009). Low scores are also observed in more scattered areas along the ABPE when TMPA V7 and TMPA RT are analyzed (lower than 0.15). Nevertheless, this relationship is slightly improved in the northern region of the Ucayali basin (~0.2).

### 4.3 Streamflow simulation

To optimize the simulation of streamflows from precipitation datasets, different parameter sets were assigned to each basin in the ABPE during calibration. Analysis by sub-basin is more reliable than assigning the same parameter set to the entire basin [Zubieta et al, 2015]. Based on sensitivity analysis of the MGB-IPH model [Collischonn et al, 2007], six parameters were selected for calibration:  $Wm_i$  (mm),  $b_i$  (-),  $Kint$  (mm.d<sup>-1</sup>),  $Kbas_i$  (mm.d<sup>-1</sup>),  $CS_i$  (-) and  $CI_i$  (-), where  $Wm$  represents water retained in the soil, which influences the evaporation process over time;  $Kint$  and  $Kbas$  control the amount of water in cases in which subsurface soil and groundwater, respectively, are saturated; and  $CS$  and  $CI$  allow for adjustment of retention time of flows [Collischonn, 2001]. To determine optimal parameters, an automatic calibration process was used in order to reduce the domain extent; a previous manual adjustment of the values was performed (Table 3). To ensure impartiality, parameter sets were calibrated separately for each precipitation dataset. Different domains were considered initially for each parameter value, and a first value, determined by manual calibration, was defined as the relative centroid for each domain. The MOCOM-UA multi-criteria global optimization algorithm

- Eliminado: -
- Con formato: Color de fuente: Texto 1
- Eliminado: with
- Con formato: Color de fuente: Texto 1
- Con formato: Color de fuente: Texto 1
- Eliminado: )
- Con formato: Color de fuente: Texto 1
- Con formato: st,Color de fuente: Texto 1, Inglés (británico)

- Eliminado: 4.2 Streamflow simulation . ... [32]
- Con formato: Fuente: +Títulos de tema (Cambria), 10 pt, Color de fuente: Texto 1
- Con formato: Fuente: +Títulos de tema (Cambria), 10 pt, Color de fuente: Texto 1
- Eliminado: The analysis
- Con formato: Fuente: +Títulos de tema (Cambria), 10 pt, Color de fuente: Texto 1

[Yapo et al., 1998] was then used to find optimal solutions for six parameters. This process results in an effective and efficient search on the Pareto optimum space [Boyle et al., 2000]. To analyze the impacts on the calibrated parameters, average parameters were calculated for precipitation datasets and HRU (Table 4).

The results of the calibration process indicate that overestimation by TMPA RT compared to observed rainfall (PLU), GPM-IMERG and TMPA V7 (Fig. 2a) in several months is consistent with a mean increase in  $Wm$  (+53%, +6%, +15% respectively), along with a predominantly mean decrease in  $Kbas$  (-18%, -39% and -16% respectively) and  $Kint$  (-25%, -15%, +2%) to achieve water balance (Table 4). Meanwhile, the overestimation by PLU compared to GPM-IMERG, TMPA V7 and TMPA RT (Fig. 3a) is consistent with a mean increase in  $Wm$  (+33%, +38%, +34% respectively), along with a mean decrease in  $Kbas$  (-30%, -28% and -38% respectively) and  $Kint$  (-17%, -16%, -17%) to achieve water balance (Table 4).

Resulting simulated streamflows were compared to observations at 11 gauging stations (Fig. 1b, Table 5). The Ucayali and Huallaga basins (with greater availability of rainfall gauges) and the northern region of the ABPE (without rainfall gauge availability) were considered in the comparative analysis. In general, streamflows obtained from all satellite-based precipitation datasets show the same spatial pattern as those obtained by using PLU (Figs. 4a-b) and are similar to those obtained by Zubieta et al. [2015]. This study shows that GPM-IMERG can also be a helpful alternative source of data (similar to TMPA V7 and TMPA RT) for rainfall-runoff simulation in areas where conventional rainfall data is lacking, such as the Andean-Amazon regions of the Ucayali basin. The performance analysis over the equatorial regions does not agree well with observed streamflows (NS lower than 0.60), probably because of the lack of adequate rainfall estimates. Similar results are obtained using the TMPA V7 (Fig. 4c) and TMPA RT (Fig. 4d) satellite precipitation datasets in the hydrological modeling.

Figs. 5a-f shows the ability of the MGB-IPH model to simulate observed streamflows using TMPA V7, TMPA RT, GPM-IMERG and PLU precipitation datasets. Simulated streamflows match observations at six stations: a) Chazuta (CHA) b) Km105 (KM), c) Lagarto (LA), d) Mejorada (ME), e) Pucallpa (PU) and e) Requena (RE). The

**Eliminado:** 2015]. Simulated streamflows were compared to observations at 11 gauging stations (Fig. 1b, Table 3).

**Con formato:** Color de fuente: Texto 1

**Con formato:** Color de fuente: Texto 1

**Eliminado:** there is a lack of

**Con formato:** Color de fuente: Texto 1

**Con formato:** Color de fuente: Texto 1

**Eliminado:** also

**Con formato:** Color de fuente: Texto 1

**Eliminado:** satellite precipitation datasets

**Con formato:** Color de fuente: Texto 1

**Con formato:** Color de fuente: Texto 1

**Con formato:** Fuente:10 pt, Color de fuente: Texto 1

**Con formato:** Color de fuente: Texto 1

**Con formato:** Color de fuente: Texto 1

**Eliminado:** ,

**Con formato:** Color de fuente: Texto 1

location of each dataset on the plot quantifies how closely the modeled streamflows match observed streamflows in terms of CV, correlation coefficient and RMSD.

Con formato: Color de fuente: Texto 1

Fig. 5a shows a Taylor diagram for the Chazuta station (Huallaga basin), where modeled streamflows from the PLU dataset agree better with observed streamflows ( $r=0.84$ ,  $p<0.01$ ), RMSD error (30%) and CV of 29% than do those using data from satellite products (TMPA RT, TMPA V7 and GPM-IMERG). Analysis of the two smallest sub-basins (in the Ucayali basin) controlled at the KM (Fig. 5b) and ME (Fig. 5c) stations shows a correlation pattern of  $r \sim 0.9$  with RMSD of  $\sim 40\%$  at KM and 24-40% at ME (Fig. 5b-c). These results indicate that the streamflows from PLU and TMPA RT are more similar to the observed streamflow series mainly at ME, with RMSD lower than 30%. The streamflow series at both KM and ME have a high CV (40%-80%), due to rainfall seasonality.

Con formato: Color de fuente: Texto 1

Con formato: Color de fuente: Texto 1

Eliminado: Both

Con formato: Color de fuente: Texto 1

Con formato: Color de fuente: Texto 1

Analysis of the largest sub-basins (in the Ucayali basin) controlled at the LA, PU and RE stations shows greater similarity among them for the four streamflow series obtained from precipitation datasets (Fig. 5d-f). Their significant correlation patterns are between 0.8 and 0.9 ( $r > 0.9$  at the PU station), and RMSD is mainly between 20% and 25% (PU and RE). It should be noted that streamflow data series have a lower CV in the larger sub-basins, such as LA, with CV of 55% (drainage area of 191,400 km<sup>2</sup>); PU, with CV  $\sim$  of 42% (drainage area of 260,400 km<sup>2</sup>); and RE, with CV of  $\sim 40\%$  (drainage area of 350,200 km<sup>2</sup>). This could be due to weaker seasonality of rainfall in the northern part of the basin. For simulations using satellite-based precipitation datasets, the correlation between simulated and observed streamflows is mainly between 0.6 and 0.9, and RMSD is relatively high (20% - 40%), suggesting that a hydrological model using these datasets can represent seasonal streamflows.

Eliminado: are

Con formato: Color de fuente: Texto 1

Eliminado: It should be noted

Con formato: Color de fuente: Texto 1

Eliminado: As for

Con formato: Color de fuente: Texto 1

The PLU dataset used as input to the hydrological model produced good results at the KM 105 (NS = 0.82 and  $\Delta V = 0.33\%$ ) (Fig. 6a), Mejorada (NS = 0.89 and  $\Delta V = 4.2\%$ ) and Lagarto (NS = 0.74 and  $\Delta V = -9.52\%$ ) stations in the Ucayali basin. This indicates its ability to represent extreme values (peak flow) with a low percentage of relative volume error ( $\Delta V < 10\%$ ). However, the model's performance is low at the Pucallpa and Requena stations (NS < 0.51 and  $\Delta V \sim 10\%$ ), where its predictions are not accurate. The low performance (NS < 0.60) is associated with drainage areas greater than the approximate threshold value of 200,000 km<sup>2</sup> in the Ucayali basin. This could be due to greater uncertainty in the spatial distribution of rainfall in the Ucayali and Huallaga basins (northern region of the ABPE), because there are fewer rainfall stations in these regions. The Peruvian Andes are currently more instrumented than the Amazon regions (see Fig. 1b).

Con formato: Color de fuente: Texto 1

Eliminado:

Con formato: Color de fuente: Texto 1

To analyze the usefulness of the GPM-IMERG datasets for hydrological modeling, hydrographs for the Ucayali basin monitored at Km 105 station (Fig. 6b) were analyzed, with streamflows from the PLU, TMPA V7 and TMPA RT datasets also considered (Fig. 6c-d). Visual analysis of the hydrographs shows that simulated streamflows using GPM-IMERG for the selected period agree fairly well with observed streamflows for the KM 105 station. Although the Nash–Sutcliffe efficiency coefficient is generally acceptable ( $NS = 0.90$  and  $\Delta V = -0.25\%$ ), as shown in Fig. 6b, there is a slight overestimation of streamflow during the wet season, which could be due to overestimation of rainfall during that season. Other results indicate that the model's performance is minimally acceptable in comparison to observed streamflow at the Pucallpa ( $NS = 0.61$ ,  $\Delta V = -17.2\%$ ) (Fig. 6g), and Mejorada stations ( $NS = 0.61$ ,  $\Delta V = -18.5\%$ ). For the other stations, performance within the basin is less than zero.

Similar results were observed using TMPA V7 and TMPA RT, which reproduce the seasonal streamflow regime with similar performance at the KM 105 ( $NS = 0.80$  and  $\Delta V = -2.78\%$ ,  $NS = 0.68$  and  $\Delta V = 11.5\%$ , respectively) (Figs. 6c-d) and Pucallpa ( $NS = 0.60$  and  $\Delta V = -17.8\%$ ,  $NS = 0.89$  and  $\Delta V = -8.3\%$ , respectively) stations in the Ucayali basin (Figs. 6h-i).

## 5 Concluding Remarks

Three satellite-based precipitation datasets (GPM-IMERG, TMPA V7, and TMPA RT) were evaluated against a rain-gauge-based dataset (PLU) obtained by spatial interpolation over the Amazon basin of Peru and Ecuador. Each dataset was used as input for the MGB-IPH hydrological model to simulate streamflows for a 16-month period (from March 2014 to June 2015) in the Ucayali, Huallaga, Marañón, Napo, Amazonas and Solimões river basins.

GPM-IMERG and TMPA V7 show high temporal and spatial similarity to PLU in the Ucayali basin, but they tend to underestimate PLU in the Huallaga basin during the wet season of the 2014-2015 period. TMPA RT tends to overestimate for the Ucayali basin, compared to other precipitation datasets (PLU, TMPA V7, GPM-IMERG), while it is more similar to other satellite-based precipitation datasets (TMPA V7, GPM-IMERG) in the Huallaga basin.

Eliminado: ability

Eliminado: in

Con formato: Color de fuente: Texto 1

Eliminado: were analyzed

Con formato: Color de fuente: Texto 1

Con formato: Color de fuente: Texto 1

Con formato: Color de fuente: Texto 1

Eliminado: 6b), for comparison,

Con formato: Color de fuente: Texto 1

Con formato: Color de fuente: Texto 1

Eliminado: were

Con formato: Color de fuente: Texto 1

Eliminado: streamflow

Con formato: Color de fuente: Texto 1

Con formato: Color de fuente: Texto 1

Eliminado: this wet

Con formato: Color de fuente: Texto 1

Con formato: Espacio Detrás: 0 pto, Esquema numerado + Nivel: 1 + Estilo de numeración: 1, 2, 3, ... + Empezar en: 4 + Alineación: Izquierda + Alineación: 0 cm + Sangría: 0.63 cm

Con formato: Color de fuente: Texto 1

Eliminado: s

Con formato: Color de fuente: Texto 1

Eliminado: with

Con formato: Color de fuente: Texto 1

The GPM-IMERG dataset shows greater similarity to TMPA V7 than TMPA RT. This indicates that GPM-IMERG estimates are more similar to TMPA V7 both spatially and temporally when used as input for hydrological modeling over Andean and Amazonian basins. On average, rain event detection coefficients also suggest that GPM-IMERG, TMPA V7 and TMPA RT are similar to PLU in the number of rain events correctly detected (~20%) for the Ucayali and Huallaga basins. Analysis of rain events from pixel value comparing PLU and estimated daily rainfall (GPM-IMERG, TMPA V7 and TMPA RT) suggests a low capacity for detection. This does not imply that they are not useful for hydrological modeling, because rain events not correctly detected for a region or a day could be correctly detected on another day or in nearby regions, compensating for the estimation of rainfall amount over large regions.

- Eliminado: s
- Con formato: Color de fuente: Texto 1
- Eliminado: with
- Con formato: Color de fuente: Texto 1
- Con formato: Color de fuente: Texto 1
- Con formato: Color de fuente: Texto 1

Con formato: Color de fuente: Texto 1

In general, the performance of the model when using the GPM-IMERG dataset indicates that these data are useful for estimating observed streamflows in Andean-Amazonian regions (Ucayali basin, southern regions of the Peruvian and Ecuadorian Amazon Basin). These results are similar to those obtained from TMPA V7 estimates by Zubieta et al. [2015] for the 2003-2009 period. Streamflows obtained from the GPM-IMERG, TMPA V7 and TMPA RT datasets show the same spatial pattern as those obtained by using PLU (low and high performance in the northern and southern regions of the ABPE, respectively). The ability to represent seasonal streamflows in the southern region using these four precipitation datasets is validated with statistical evaluation.

- Con formato: Color de fuente: Texto 1
- Con formato: No ajustar espacio entre texto latino y asiático, No ajustar espacio entre texto asiático y números
- Con formato: Color de fuente: Texto 1
- Eliminado: s
- Con formato: Color de fuente: Texto 1
- Con formato: Color de fuente: Texto 1
- Eliminado: ,
- Eliminado: ,
- Con formato: Color de fuente: Texto 1
- Con formato: Color de fuente: Texto 1
- Eliminado: for
- Con formato: Color de fuente: Texto 1
- Eliminado: corroborated by
- Con formato: Color de fuente: Texto 1
- Eliminado: . Low performance of the model in the southern region is mainly related to the lack of adequate rainfall estimates, because it is consistent with estimated streamflows
- Con formato: Color de fuente: Texto 1

It is important to note that the advantages of GPM-IMERG over TMPA-V7 for estimating streamflows, such as temporal resolution (30 minutes compared to 3 hours, respectively), have not yet been fully analyzed. The use of sub-daily rainfall data can be potentially useful for simulating discharge in the Andean rivers, where short convective rainfall episodes are more relevant for hydrological variability. In this study, precipitation and streamflows were analyzed at a daily time step. Further flash flood modeling at smaller scales would reveal the effects of sub-diurnal differences between datasets. Errors in streamflow simulations are mostly associated with input data uncertainty, including rainfall, limited representations of physical processes in models, and parameters such as DEM and HRUs. Nevertheless, results show that it is possible to employ remote sensing data in large-scale hydrological models for streamflow simulations.

Con formato: Color de fuente: Texto 1

Con formato: Color de fuente: Texto 1

## Acknowledgements

The authors would like to thank SENAMHI for providing observed precipitation data series and the SO-HYBAM observatory for providing discharge data [www.ore-hybam.org]. The authors also acknowledge GSFC/DAAC and PMM [NASA] for providing TMPA [http://disc.sci.gsfc.nasa.gov/ /data/TRMM/Gridded/] and GPM-IMERG [https://pmm.nasa.gov/data-access/downloads/gpm] datasets respectively. Finally, RZ and JCE wish to acknowledge the PNICP-Peru for providing funds through Contract 397-PNICP-PIAP-2014.

## References

[Boyle, D.P., Gupta, H.V., Sorooshian, S.: Toward improved calibration of hydrologic models: combining the strengths of manual and automatic methods. \*Water Resources Research\* 36 \(12\), 3663–3674, 2000.](#)

[Brunet-Moret, Y.: Homogénéisation des précipitations. \*Cahiers ORSTOM, Série Hydrologie\* 16: 3–4, 1979.](#)

Con formato: Color de fuente: Texto 1

Con formato: Color de fuente: Texto 1, Inglés (americano)

Con formato: Color de fuente: Texto 1

[Collischonn, W., Allasia, D.G., Silva, B.C., Tucci, C.E.M.: The MGB-IPH model for large-scale rainfall-runoff modeling, \*J. Hydrol. Sci.\* 52, 878–895, doi: 10.1623/hysj.52.5.878, 2007.](#)

Con formato: Color de fuente: Texto 1, Inglés (americano)

Con formato: Color de fuente: Texto 1

[Collischonn, B., Collischonn, W., Tucci, C.: Daily hydrological modeling in the Amazon basin using TRMM rainfall estimates, \*J. Hydrol.\* 360, 207–216, 10.1016/j.jhydrol.2008.07.032, 2008.](#)

Con formato: Color de fuente: Texto 1, Inglés (americano)

Con formato: Color de fuente: Texto 1

Con formato: Color de fuente: Texto 1, Inglés (americano)

[Espinoza, J.C., Ronchail, J., Guyot, J.L., Cochonneau, G., Filizola, N.P., Lavado, C., De Oliveira, E., Pombosa, R., Vauchel P.: Spatio-Temporal rainfall variability in the Amazon basin countries \(Brazil, Peru, Bolivia, Colombia and Ecuador\), \*I.J. of Climatology\* 29\(11\): 1574–1594, doi:10.1002/joc.1791, 2009.](#)

Con formato: Color de fuente: Texto 1

Con formato: Color de fuente: Texto 1, Inglés (americano)

Con formato: Color de fuente: Texto 1

[Espinoza, J.C., Ronchail, J., Guyot, J.L., Junquas, C., Vauchel, P., Lavado, W.S., Drapeau, G., Pombosa, R.: Climate variability and extremes drought in the upper Solimões River \(Western Amazon Basin\): Understanding the exceptional 2010 drought, \*Geophys. Res. Lett.\*, 38, L13406, doi: 10.1029/2011GL047862, 2011.](#)

Con formato: Color de fuente: Texto 1, Inglés (americano)

Con formato: Color de fuente: Texto 1

Con formato: Color de fuente: Texto 1, Inglés (americano)

Con formato: Color de fuente: Texto 1

Con formato: Color de fuente: Texto 1, Inglés (americano)

[Espinoza, J.C., Ronchail, J., Guyot, J. L., Junquas, C., Drapeau, G., Martinez, J.M., Santini, W., Vauchel, P., Lavado, W., Ordoñez, J., and Espinoza, R.: From drought to flooding: understanding the abrupt 2010–11 hydrological annual cycle in the Amazonas River and tributaries, Environ. Res. Lett. 7 024008, doi:10.1088/1748-9326/7/2/024008, 2012.](#)

Con formato: Color de fuente: Texto 1

Espinoza, J.C., Ronchail, J., Frappart, F., Lavado, W., Santini, W., Guyot, J.L. : The major floods in the Amazonas River and tributaries (Western Amazon basin) during the 1970 – 2012 period: A focus on the 2012 flood, *Journal of Hydrometeorology*, 14, 1000-1008, doi:10.1175/JHM-D-12-0100.1, 2013.

Con formato: Color de fuente: Texto 1, Inglés (americano)

Con formato: Color de fuente: Texto 1

[Espinoza, J.C., Marengo, J.A., Ronchail, J., Molina, J., Noriega, L., Guyot, J.L.: The extreme 2014 flood in south-western Amazon basin: The role of tropical-subtropical south Atlantic SST gradient, Environm. Res. Lett. 9 124007, doi:10.1088/1748-9326/9/12/124007, 2014.](#)

Con formato: Color de fuente: Texto 1, Inglés (americano)

Con formato: Color de fuente: Texto 1

Espinoza, J.C., Chavez, S., Ronchail, J., Junquas, C., Takahashi, K., Lavado, W.: Rainfall hotspots over the southern tropical Andes: Spatial distribution, rainfall intensity and relations with large-scale atmospheric circulation, *Water Resources Res.* 51, doi:10.1002/2014WR016273, 2015.

Getirana, A.C.V., Espinoza, J.C., Ronchail, J., Rotunno, O.: Assessment of different precipitation datasets and their impacts on the water balance of the Negro River basin, *J. Hydrol.* 404 (3–4), 304–322, doi:10.1016/j.jhydrol.2011.04.037, 2011.

Con formato: Color de fuente: Texto 1, Inglés (americano)

Con formato: Color de fuente: Texto 1

Gloor, MRJW., Brienens, D., Galbraith, TR., Feldpausch, J., Schöngart, W., Guyot, JL., Espinoza, JC., Lloyd, J., Phillips, O.L.: Intensification of the Amazon hydrological cycle over the last two decades, *Geophys. Res. Lett.* 40: 1729–1733, doi: 10.1002/grl.50377, 2013.

[Guimberteau, M., Drapeau, G., Ronchail, J., Sultan, B., Polcher, J., Martinez, J.M., Prigent, C., Guyot, J.L., Cochonneau, G., Espinoza, J.C., Filizola, N., Fraizy, P., Lavado, W., De Oliveira, E., Pombosa, R., Noriega, L., Vauchel, P.: Discharge simulation in the sub-basins of the Amazon using ORCHIDEE forced by new datasets. \*Hydrol. Earth Syst. Sci.\* 16, 911–935, 2012.](#)

[Hiez, G. : L'homogénéité des données pluviométriques, Cahier ORSTOM, série Hydrologie 14: 129–172, 1977.](#)

Con formato: Color de fuente: Texto 1

Huffman, G., Adler, R., Bolvin, D., Gu, G., Nelkin, E., Bowman, K., Hong, Y., Stocker, E., Wolff, D.: The TRMM Multisatellite Precipitation Analysis (TCMA): quasi-global, multiyear, combined- sensor precipitation estimates at fine scales, *Journal of Hydrometeorology* 8, 38–55, doi:10.1.1.532.5634, 2007.

Huffman, G.J., Bolvin, D.T., Nelkin, E.J.: Day 1 IMERG Final Run Release Notes; NASA Goddard Earth Sciences Data and Information Services Center: Greenbelt, MD, USA, 2015.

Kanamitsu, M., Ebisuzaki, W., Woolen, J., Yang, S.K., Hnilo, J.J., Fiorino, M., Potter, G.L.: NCEP-DOE AMIP-II Reanalysis (R-2). *Bull. Amer. Meteor. Soc.* 83, 1631–1643, doi:10.1175/BAMS-83-11-1631, 2002.

Con formato: Fuente:Color de fuente: Texto 1, Inglés (americano)

Killeen, T. J., Douglas, M., Consiglio, T., Jorgensen, P. M. and Mejia J.: Dry spots and wet spots in the Andean hotspot, *J. Biogeogr.*, 34(8), 1357–1373, doi:10.1111/j.1365-2699.2006.01682.x, 2007

Con formato: Color de fuente: Texto 1

Con formato: Izquierda, Sangría: Izquierda: 0 cm, Sangría francesa: 1.27 cm, Ajustar espacio entre texto latino y asiático, Ajustar espacio entre texto asiático y números

Kouwen, N. & Mousavi, S. F.: WATFLOOD/SPL9: Hydrological model and flood forecasting system. In: *Mathematical Models of Large Watershed Hydrology* (ed. by V. P. Singh & D. K. Frevert), Water Resources Publications. Highlands Ranch. Colorado, USA, 2002.

Con formato: Color de fuente: Texto 1

Laraque, A., Ronchail, J., Cochonneau, G., Pombosa, R., Guyot, J.L.: Heterogeneous distribution of rainfall and discharge regimes in the Ecuadorian Amazon basin, *Journal of Hydrometeorology* 8: 1364–1381, doi:10.1175/2007JHM784.1, 2007.

Lavado, W., Labat, D., Ronchail, J., Espinoza, J.C., Guyot, J.L.: Trends in rainfall and temperature in the Peruvian Amazon-Andes basin over the last 40 years (1965-2007), *Hydrological Processes*. doi: 10.1002/hyp.9418, 2012.

Liu, Z.: Comparison of Integrated Multisatellite Retrievals for GPM (IMERG) and TRMM Multisatellite Precipitation Analysis (TMPA) monthly precipitation products: Initial results, *J. Hydrometeor.*, 17, 777–790, doi:10.1175/JHM-D-15-0068.1, 2016.

Marengo, J. A., Nobre, C. A., Tomasella, J., Oyama, M., Sampaio, G., Camargo, H., Alves, L.: "The Drought of Amazonia in 2005," *Journal of Climate*, Vol. 21, No. 3, 495-516. doi:10.1175/2007JCLI1600.1, 2008

Con formato: Color de fuente: Texto 1, Inglés (americano)

Marengo, J. A., Tomasella, J., Alves, L., Soares, W. and Rodriguez, D. A.: The Drought of 2010 in the Context of Historical Droughts in the Amazon Region, *Geophysical Research Letters*, Vol. 38, No. 12, 2011, pp. 1-5, doi:10.1029/2011GL047436, 2011.

Con formato: Color de fuente: Texto 1

Con formato: Fuente:Color de fuente: Texto 1, Inglés (americano)

Paiva, R. C. D., Buarque, D. C., Collischonn, W., Bonnet, M.P., Frappart, F., Calmant, S. and Mendes, C. A. B. : Large scale hydrologic and hydrodynamic modeling of the Amazon River basin. *Water Resour Res.*, 49, 1226–1243, doi:10.1002/wrcr.20067, 2013.

Con formato: Color de fuente: Texto 1

Schwaller, M. R. and K. R. Morris.: A Ground Validation Network for the Global Precipitation Measurement Mission, *J. Atmos. Oceanic Technol.*, 28, 301–319, doi: 10.1175/2010jtecha1403.1, 2011.

Con formato: Fuente:Color de fuente: Texto 1, Inglés (americano)

Tang, G., Z. Zeng, D. Long, X. Guo, B. Yong, W. Zhang, and Y. Hong.: Statistical and hydrological comparisons between TRMM and GPM level-3 products over a midlatitude basin: Is day-1 IMERG a good successor for TMPA 3B42V7?, *J. Hydrometeorol.*, 17, 121–137, doi:10.1175/jhm-d-15-0059.1, 2016.

Con formato: Color de fuente: Texto 1

Taylor, K. E.: Summarizing multiple aspects of model performance in a single diagram, *J. Geophys. Res.*, 106(D7), 7183–7192, doi: 10.1029/2000JD900719, 2011.

Wilks, D.S., 1995. *Statistical methods in Atmospheric sciences*. Academic press, San Diego, CA, p. 467.

Yapo, P.O., Gupta, H.V., Sorooshian, S.: Multi-objective global optimization for hydrologic models. *Journal of Hydrology* 204, 83–97, 1998.

Con formato: Color de fuente: Texto 1

Zubieta, R., Geritana, A., Espinoza, J.C. and Lavado W.: Impacts of Satellite-based Precipitation Datasets on Rainfall-Runoff Modeling of the Western Amazon Basin of Peru and Ecuador, *Journal of Hydrology*, doi:10.1016/j.jhydrol.2015.06.064, 2015.

Zubieta, R., Saavedra, M., Silva, Y., Giraldez, L.: Spatial analysis and temporal trends of daily precipitation concentration in the Mantaro River basin - Central Andes of Peru, *Stochastic Environmental Research and Risk Assessment*. DOI :10.1007/s00477-016-1235-5, 2016.

Zulkafli, Z., Buytaert, W., Onof, C., Manf, B., Tarnavsky, E., Lavado, W., and Guyot, J. L.: A Comparative Performance Analysis of TRMM 3B42 (TMPA) Versions 6 and 7 for Hydrological Applications over Andean–Amazon River Basins, *J. Hydrometeorol.*, 15, 581–592, doi: 10.1175/JHM-D-13-094.1, 2014.

**Table 1.** Characteristics of streamflow gauging stations in the Amazon basin of Peru and Ecuador: Altitude, river, drainage area, annual mean streamflow (Q mean), maximum streamflow (Q max) and minimum streamflow (Q min) in m<sup>3</sup>/s.

N	Station	Altitude	River	Area (Km 2)	Q medio		
					(m <sup>3</sup> /s)	Q max (m <sup>3</sup> /s)	Q min (m <sup>3</sup> /s)
1	Km 105 (KM)	2275	Ucayali	9635	98	446	30
2	Mejorada (ME)	2799	Ucayali	16930	186	651	76
3	Chazuta (CHA)	226	Marañon	68685	3430	8921	936
4	Borja (BOR)	163	Marañon	92302	6123	13250	1931
5	Bellavista (BE)	90	Napo	100169	9338	13110	4654
6	Lagarto (LA)	200	Ucayali	191428	6194	30460	1292
7	Pucallpa (PU)	141	Ucayali	260418	10833	21830	3714
8	Requena (RE)	94	Ucayali	350215	13669	20910	4088
9	San Regis (SR)	92	Marañon	359883	20119	26610	9071
10	Tamshiyacu (TAM)	88	Amazon	682970	37380	53840	15000
11	Tabatinga (TAB)	62	Solimões	878141	45384	62190	19700

Eliminado: - ... [33]

Con formato: Color de fuente: Texto 1

**Table 2.** Summary of rain event detection coefficients.

Coefficient	Name	Equation*	Range	Optimal score
FBI	Frequency bias index	$FBI = (a+b)/(a+c)$	0 - $\infty$	1
POD	Probability of detection	$POD = a/(a+c)$	0 - 1	1
FAR	False alarm ratio	$FAR = c / (a+c)$	0 - 1	0
ETS	Equitable threat score	$ETS = (a+He)/(a+b+c-He)$	- $\infty$ to 1	1

\*  $He = (a+b) \cdot (a+c)/N$  where N is the total number of estimates

Eliminado: - ... [34]

Con formato: Color de fuente: Texto 1

Con formato: Fuente: Negrita, Color de fuente: Texto 1, Inglés (británico)

Con formato: Normal, Interlineado: sencillo

Vertical line segment on the left side of the page.

Vertical line segment on the left side of the page.

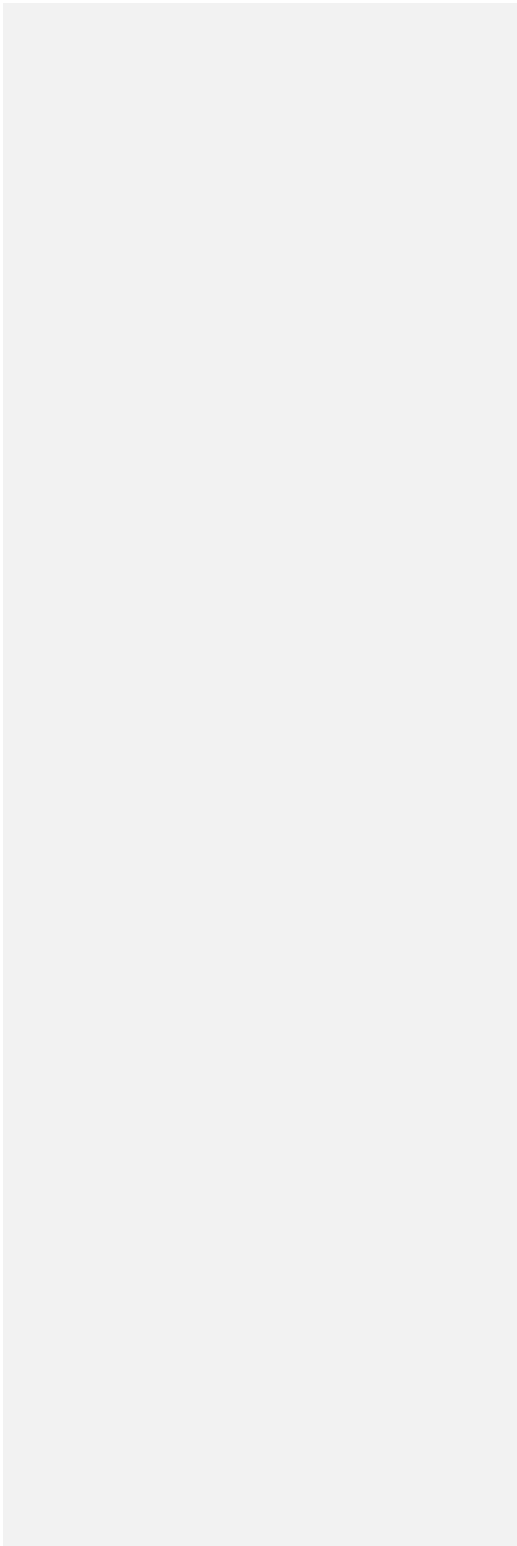


**Table 3.** Model parameters subjected to the process of automatic calibration for the Peruvian and Ecuadorian Amazon basin.

<u>Parameter</u>	<u>HRU</u>	<u>Hydrological process</u>	<u>First guess</u>	<u>Domain</u>
<u>Wm(mm)</u>	<u>Shrubs, agricultural areas/not deep soils</u>	<u>Water storage on the HRU</u>	<u>200</u>	<u>50-1200</u>
	<u>Shrubs, agricultural areas/deep soils</u>		<u>400</u>	<u>50-1200</u>
	<u>Forest/not deep soils</u>		<u>350</u>	<u>50-1200</u>
	<u>Forest/deep soils</u>		<u>600</u>	<u>50-1200</u>
	<u>Pasture/not deep soils</u>		<u>120</u>	<u>50-1200</u>
	<u>Pasture/deep soils</u>		<u>240</u>	<u>50-1200</u>
<u>Kint(mm/d)</u>	<u>Shrubs, agricultural areas/not deep soils</u>	<u>Sub - surface flow</u>	<u>80</u>	<u>50-150</u>
	<u>Shrubs, agricultural areas/deep soils</u>		<u>90</u>	<u>50-150</u>
	<u>Forest/not deep soils</u>		<u>100</u>	<u>50-150</u>
	<u>Forest/deep soils</u>		<u>120</u>	<u>50-150</u>
	<u>Pasture/not deep soils</u>		<u>70</u>	<u>50-150</u>
	<u>Pasture/deep soils</u>		<u>80</u>	<u>50-150</u>
<u>Kbas(mm/d)</u>	<u>Shrubs, agricultural areas/not deep soils</u>	<u>Groundwater flow</u>	<u>30</u>	<u>10 - 100</u>
	<u>Shrubs, agricultural areas/deep soils</u>		<u>50</u>	<u>10 - 100</u>
	<u>Forest/not deep soils</u>		<u>70</u>	<u>10 - 100</u>
	<u>Forest/deep soils</u>		<u>80</u>	<u>10 - 100</u>
	<u>Pasture/not deep soils</u>		<u>55</u>	<u>10 - 100</u>
	<u>Pasture/deep soils</u>		<u>70</u>	<u>10 - 100</u>
<u>CS</u>	<u>All</u>	<u>Surface flow</u>	<u>15</u>	<u>0.35 - 40</u>
<u>CI(-)</u>	<u>All</u>	<u>Sub-surface flow</u>	<u>120</u>	<u>1 - 200</u>
<u>b(-)</u>	<u>All</u>	<u>Variable infiltration curve</u>	<u>0.12</u>	<u>0.01 - 2</u>

**Table 4.** Values of the model mean parameters used in the *Ucayali and Huallaga basins for each rainfall datasets for the 2014-2015 period.*

Parameter	HRU	UCAYALI BASIN				HUALLAGA BASIN			
		PLU	GPM- IMERG	TMPA V7	TMPA RT	PLU	GPM- IMERG	TMPA V7	TMPA RT
Wm(mm)	<u>Shrubs, agricultural areas/not deep soils</u>	<u>268</u>	<u>351</u>	<u>294</u>	<u>373</u>	<u>100</u>	<u>60</u>	<u>65</u>	<u>60</u>
	<u>Shrubs, agricultural areas/deep soils</u>	<u>340</u>	<u>472</u>	<u>503</u>	<u>597</u>	<u>132</u>	<u>102</u>	<u>96</u>	<u>99</u>
	<u>Forest/not deep soils</u>	<u>300</u>	<u>408</u>	<u>273</u>	<u>344</u>	<u>130</u>	<u>101</u>	<u>99</u>	<u>96</u>
	<u>Forest/deep soils</u>	<u>422</u>	<u>453</u>	<u>445</u>	<u>435</u>	<u>250</u>	<u>203</u>	<u>180</u>	<u>209</u>
	<u>Pasture/not deep soils</u>	<u>144</u>	<u>350</u>	<u>261</u>	<u>321</u>	<u>101</u>	<u>60</u>	<u>66</u>	<u>59</u>
	<u>Pasture/deep soils</u>	<u>196</u>	<u>400</u>	<u>454</u>	<u>496</u>	<u>150</u>	<u>120</u>	<u>116</u>	<u>121</u>
Kint (mm/d)	<u>Shrubs, agricultural areas/not deep soils</u>	<u>141</u>	<u>216</u>	<u>151</u>	<u>151</u>	<u>190</u>	<u>161</u>	<u>163</u>	<u>152</u>
	<u>Shrubs, agricultural areas/deep soils</u>	<u>180</u>	<u>236</u>	<u>156</u>	<u>163</u>	<u>220</u>	<u>189</u>	<u>195</u>	<u>198</u>
	<u>Forest/not deep soils</u>	<u>198</u>	<u>123</u>	<u>107</u>	<u>108</u>	<u>103</u>	<u>162</u>	<u>155</u>	<u>160</u>
	<u>Forest/deep soils</u>	<u>200</u>	<u>134</u>	<u>108</u>	<u>113</u>	<u>120</u>	<u>208</u>	<u>199</u>	<u>220</u>
	<u>Pasture/not deep soils</u>	<u>150</u>	<u>110</u>	<u>119</u>	<u>122</u>	<u>121</u>	<u>160</u>	<u>151</u>	<u>150</u>
	<u>Pasture/deep soils</u>	<u>180</u>	<u>113</u>	<u>126</u>	<u>128</u>	<u>132</u>	<u>193</u>	<u>201</u>	<u>190</u>
Kbas (mm/d)	<u>Shrubs, agricultural areas/not deep soils</u>	<u>103</u>	<u>121</u>	<u>89</u>	<u>93</u>	<u>55</u>	<u>70</u>	<u>72</u>	<u>80</u>
	<u>Shrubs, agricultural areas/deep soils</u>	<u>113</u>	<u>123</u>	<u>100</u>	<u>103</u>	<u>61</u>	<u>90</u>	<u>94</u>	<u>100</u>
	<u>Forest/not deep soils</u>	<u>53</u>	<u>134</u>	<u>59</u>	<u>53</u>	<u>44</u>	<u>70</u>	<u>69</u>	<u>80</u>
	<u>Forest/deep soils</u>	<u>62</u>	<u>25</u>	<u>69</u>	<u>62</u>	<u>63</u>	<u>90</u>	<u>88</u>	<u>100</u>
	<u>Pasture/not deep soils</u>	<u>64</u>	<u>112</u>	<u>66</u>	<u>64</u>	<u>46</u>	<u>70</u>	<u>76</u>	<u>80</u>
	<u>Pasture/deep soils</u>	<u>74</u>	<u>113</u>	<u>71</u>	<u>71</u>	<u>63</u>	<u>90</u>	<u>66</u>	<u>100</u>

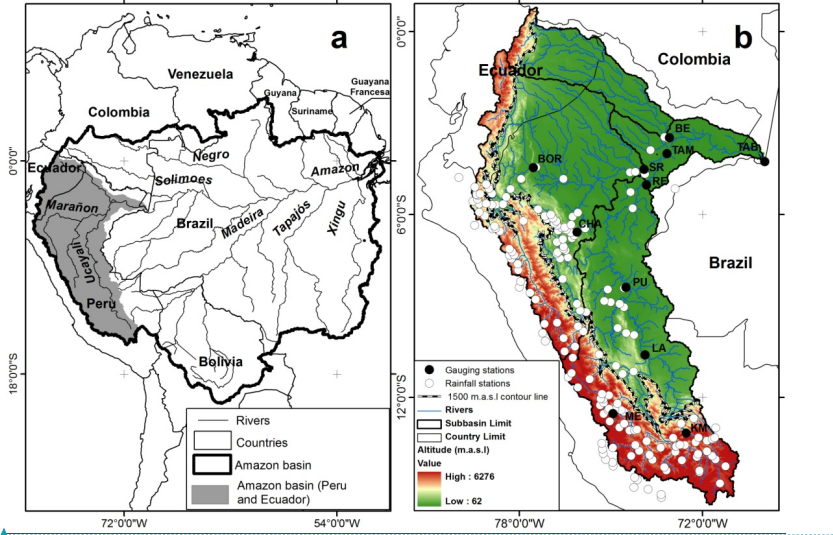
CS	All	18	16	17	17	2.6	2.4	2.6	2.5
CI(-)	All	112	111	118	111	111	133	135	132
b(-)	All	0.13	0.17	0.15	0.12	0.12	0.15	0.14	0.14

**Table 5.** Summary of modeling results at 11 gauging stations in the Amazon basin of Peru and Ecuador (to Tabatinga station in Brazil).

N	River	Station	OBSERVED RAINFALL (PLU)		GPM-IMERG		TMPA V7		TMPA RT	
			NS	Δ V	NS	Δ V	NS	Δ V	NS	Δ V
			1	Ucayali	Km 105 (KM)	0.82	0.33	0.90	-0.25	0.80
2	Ucayali	Mejorada (ME)	0.89	4.2	0.61	-18.5	0.61	-17.01	0.75	-6.49
3	Ucayali	Chazuta (CHA)	0.37	-18.27	-0.26	-31.96	-0.37	-33.51	-0.02	-29.55
4	Ucayali	Borja (BOR)	----	----	-3.94	-47.98	-3.09	-42.39	-3.91	-47.53
5	Ucayali	Bellavista (BE)	----	----	-2.17	-7.14	-18.24	-32.64	-20.93	-35.46
6	Marañon	Lagarto(LA)	0.74	-9.52	0.71	-0.13	0.80	-0.49	0.81	-0.18
7	Marañon	Pucallpa (PU)	0.48	-8.1	0.61	-17.2	0.60	-17.80	0.89	-8.3
8	Marañon	Requena (RE)	0.51	-10.6	-3.75	-23.59	-7.71	-33.28	-5.33	-23.32
9	Napo	San Regis (SR)	----	----	-5.40	-24.82	-5.68	-25.59	-4.90	-24.72
10	Amazon	Tamshiyacu (TAM)	----	----	-24.51	-32.22	-33.32	-37.57	-28.19	-33.19
11	Solimões	Tabatinga (TAB)	----	----	-3.85	-10.28	-12.88	-19.51	-5.21	-10.74

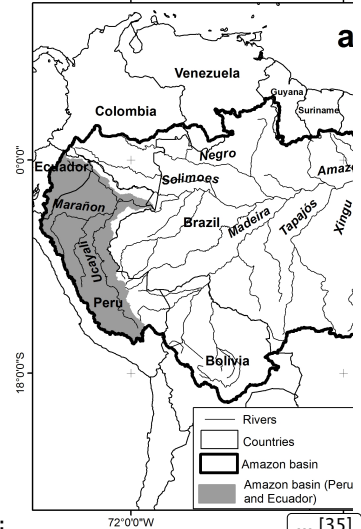
Eliminado: Table 3.

Con formato: Color de fuente: Texto 1

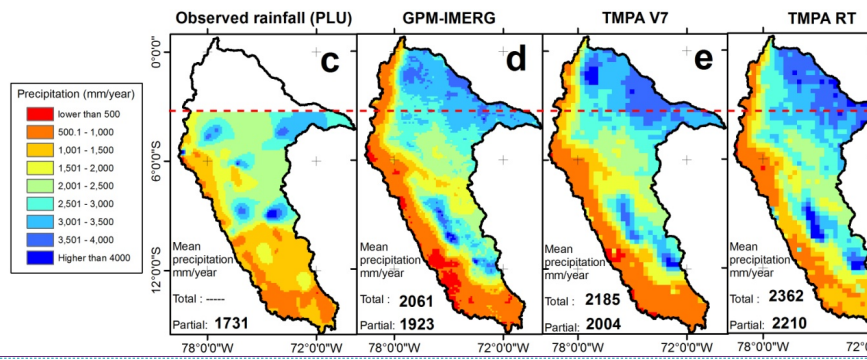


Con formato: Fuente:10 pt, Color de fuente: Texto 1

Con formato: Fuente:10 pt, Color de fuente: Texto 1



Eliminado: ... [35]



Con formato: Fuente:10 pt, Color de fuente: Automático

Con formato: Fuente:10 pt, Color de fuente: Automático

Con formato: Color de fuente: Texto 1

Con formato: Color de fuente: Texto 1, Inglés (americano)

Con formato: Color de fuente: Texto 1

Con formato: Color de fuente: Texto 1, Inglés (americano)

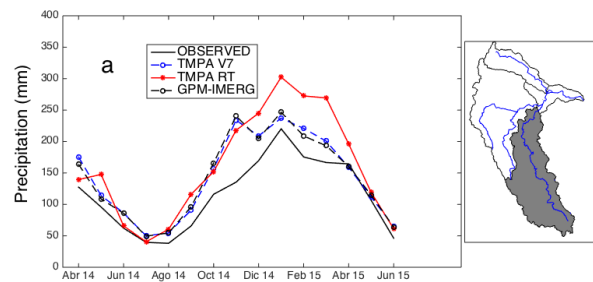
Con formato: Color de fuente: Texto 1

Figure 1. (a) Location of the Amazon basin in South America, (b) the Western Amazon basin, gauging and rainfall stations used in this work, intermittent line represents main isohypse 1500 m.a.s.l. Total annual

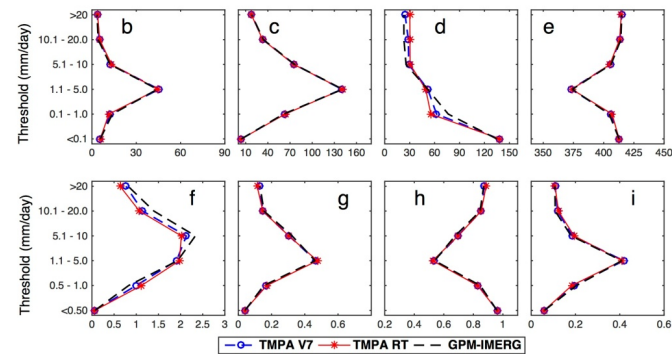
precipitation estimated from (c) observed rainfall-PLU, (d) GPM-IMERG, (e) TMPA V7, (f) TMPA RT over the Amazon basin of Peru and Ecuador. ▲

Con formato: Color de fuente: Texto 1, Inglés (americano)

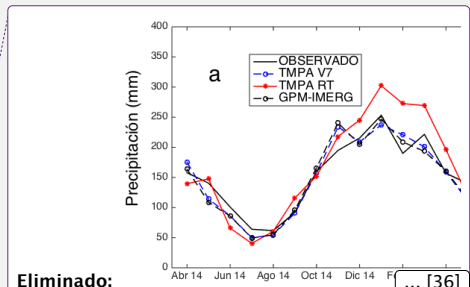
Con formato: Color de fuente: Texto 1



Con formato: Fuente:10 pt, Color de fuente: Texto 1



Con formato: Fuente:10 pt, Color de fuente: Texto 1



Eliminado:

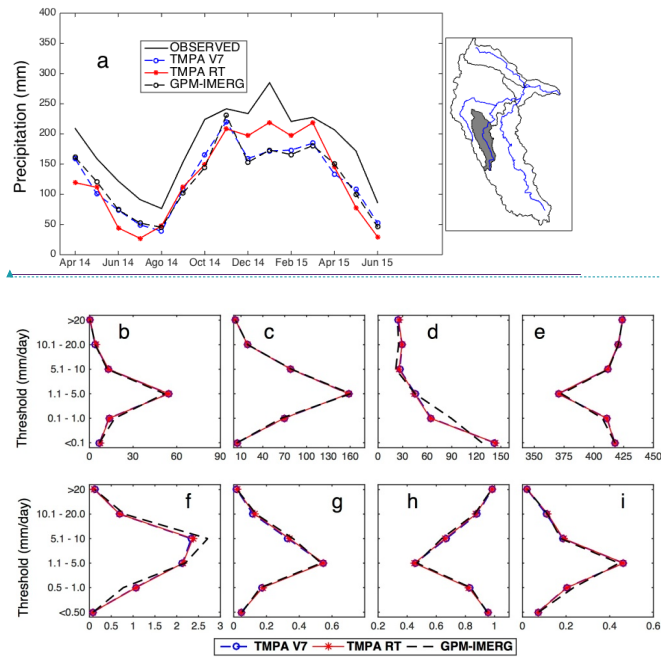
Con formato: Fuente:10 pt

Con formato: Fuente:10 pt

Con formato: Color de fuente: Texto 1

**Figure 2.** (a) Basin-average monthly rainfall for each precipitation dataset in the Ucayali basin up to Requena station, (b) the number of observed rain events correctly detected, (c) the number of observed rain events not correctly detected, (d) the number of rain events detected but not observed (false alarms), (e) the sum of

cases when neither observed nor detected rain events occurred, **(f)** coefficient frequency bias index – FBI, **(g)** probability of detection-POD, **(h)** false alarm ratio – FAR, and **(i)** equitable threat score-ETS.



Con formato: Fuente:10 pt, Color de fuente: Texto 1

Con formato: Fuente:10 pt, Color de fuente: Texto 1

**Figure 3.** **(a)** Average monthly rainfall for each precipitation dataset in the Huallaga basin up to the Chazuta station, **(b)** the number of observed rain events correctly detected, **(c)** the number of observed rain events not correctly detected, **(d)** the number of rain events detected but not observed (false alarms), **(e)** the sum of cases when neither observed nor detected rain events occurred, **(f)** coefficient frequency bias index – FBI, **(g)** probability of detection-POD, **(h)** false alarm ratio – FAR, and **(i)** equitable threat score-ETS.

Eliminado: - ... [37]

Con formato: Fuente:10 pt

Con formato: Fuente:10 pt

Con formato: Color de fuente: Texto 1

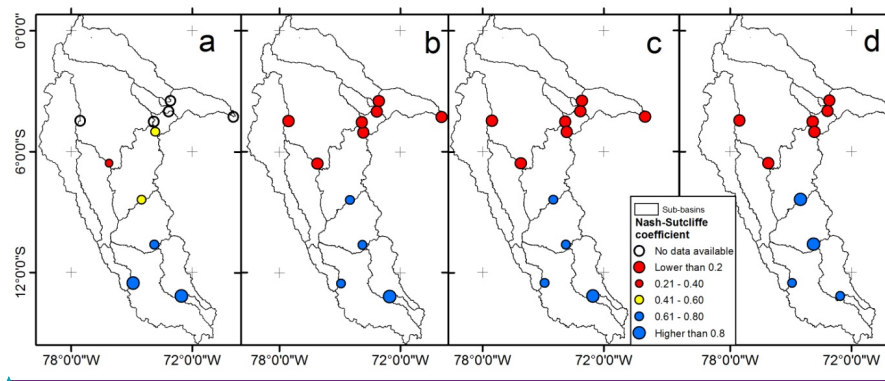
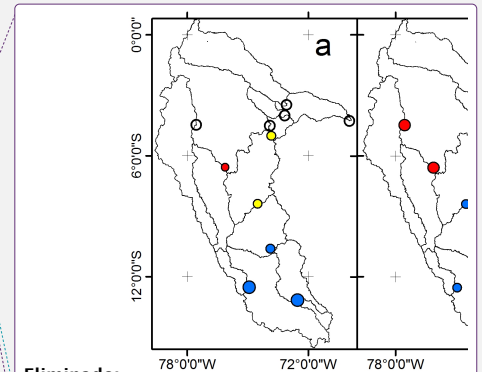


Figure 4. Nash-Sutcliffe efficiency coefficients map for simulations using: (a) Observed Rainfall (PLU), (b) GPM-IMERG, (c) TMPA V7 and (d) TMPA RT rainfall data.

Con formato: Fuente:10 pt, Color de fuente: Texto 1



Eliminado:

Con formato: Fuente:10 pt

Con formato: Color de fuente: Texto 1

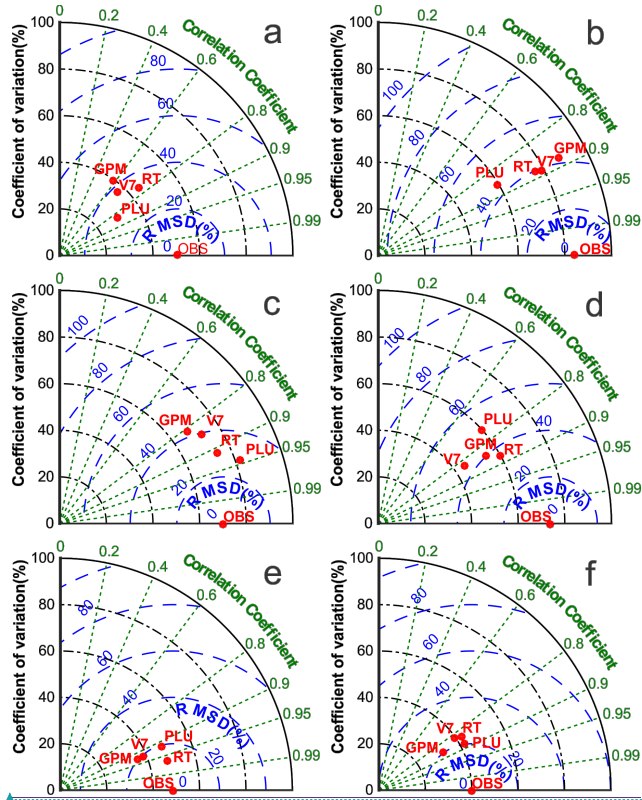
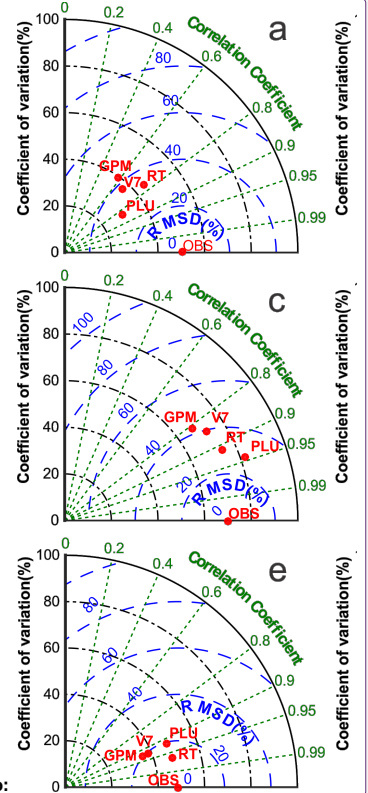


Figure 5. Taylor diagrams displaying a statistical comparison (coefficient of variation (%), the root mean square difference (%) and correlation coefficient) between observed streamflows and modeled streamflows from four precipitation datasets (TMPA V7 (V7), TMPA RT (RT), GPM-IMERG (GPM), observed rainfall (PLU))

Con formato: Fuente:10 pt, Color de fuente: Texto 1

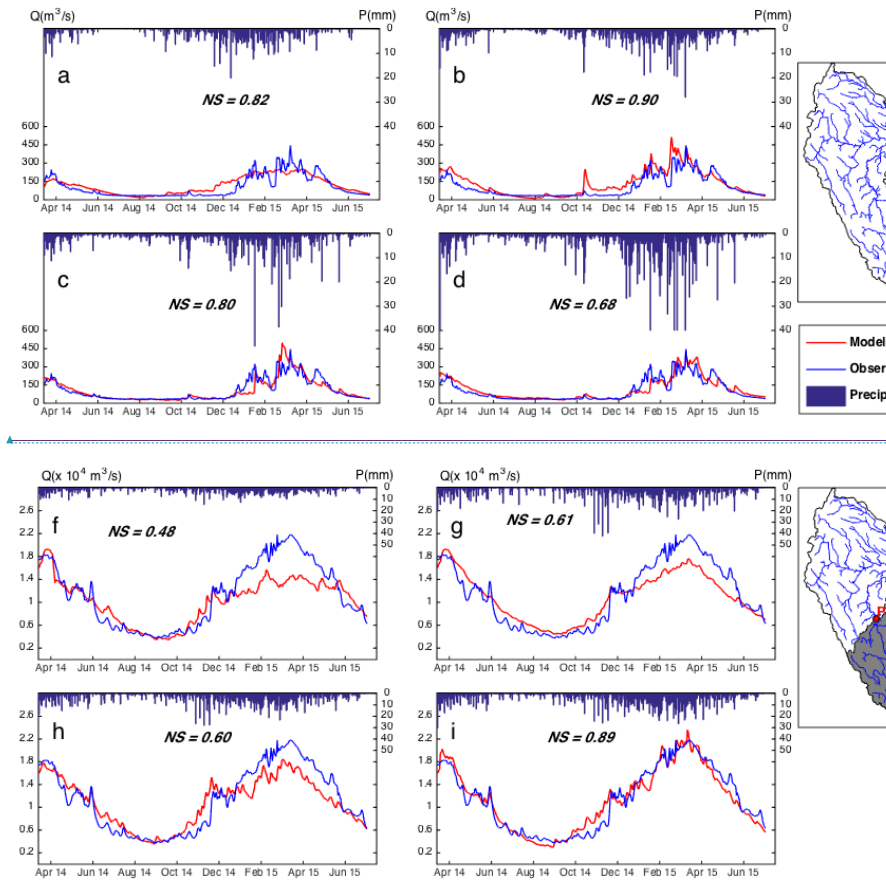


Eliminado:

Con formato: Fuente:10 pt

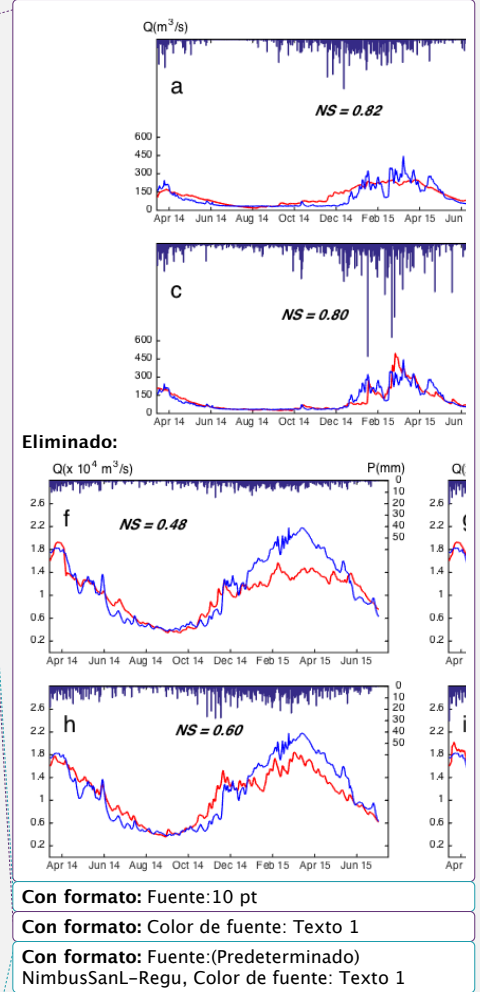
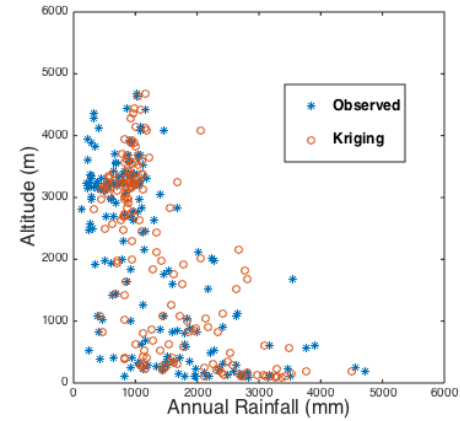
Con formato: Color de fuente: Texto 1

for six basins controlled at stations: **a)** Chazuta (CHA), **b)** Km105 (KM), **c)** Mejorada (ME), **d)** Lagarto (LA), **e)** Pucallpa (PU), and **f)** Requena (RE).

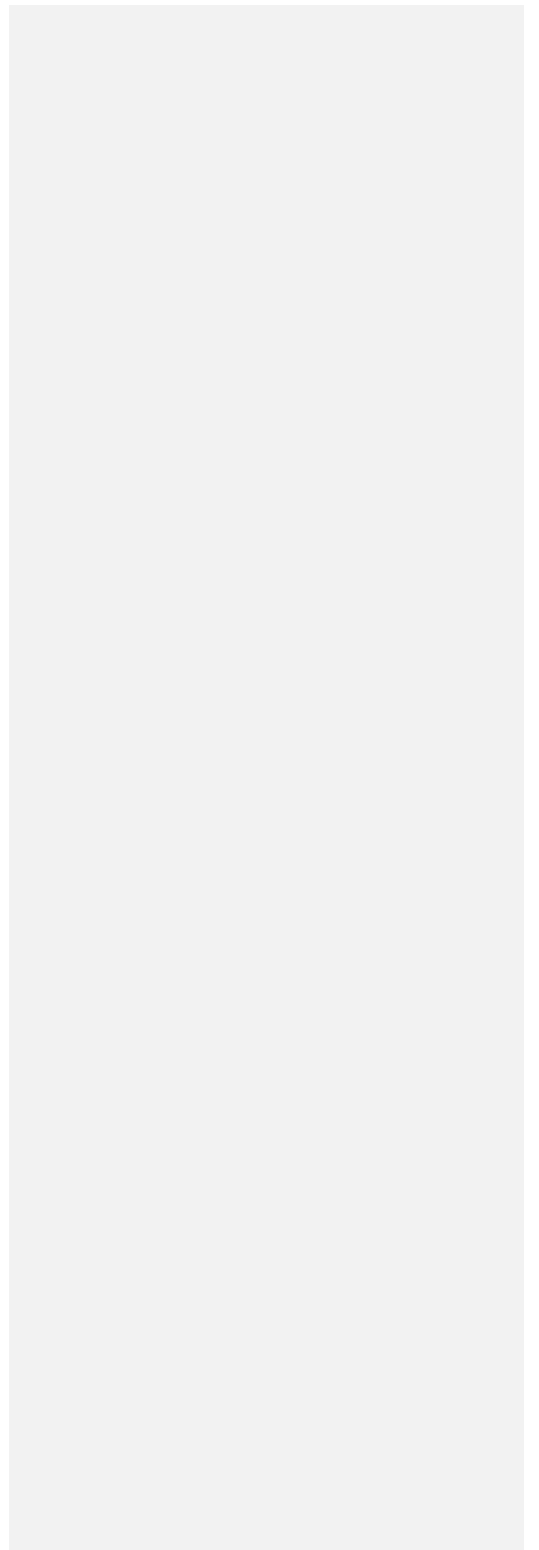


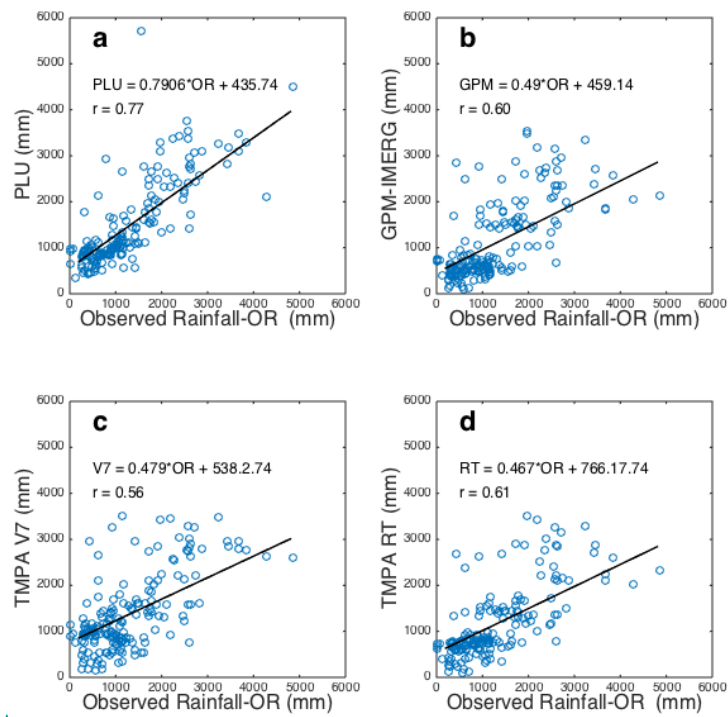
Con formato: Fuente:10 pt, Color de fuente: Texto  
1

**Figure 6.** Observed and simulated streamflow hydrographs at KM 105 station from March 12, 2014, to June 30, 2015, using precipitation datasets: **(a)** Observed rainfall, **(b)** GPM-IMERG, **(c)** TMPA V7, and **(d)** TMPA RT, **(e)** Location of the drainage area controlled at the KM station. Observed and simulated streamflow hydrographs at the Pucallpa station from March 12, 2014, to June 30, 2015, using precipitation datasets: **(f)** Observed rainfall, **(g)** GPM-IMERG, **(h)** TMPA V7, **(i)** TMPA RT; **(j)** Location of the drainage area controlled at the Pucallpa station.



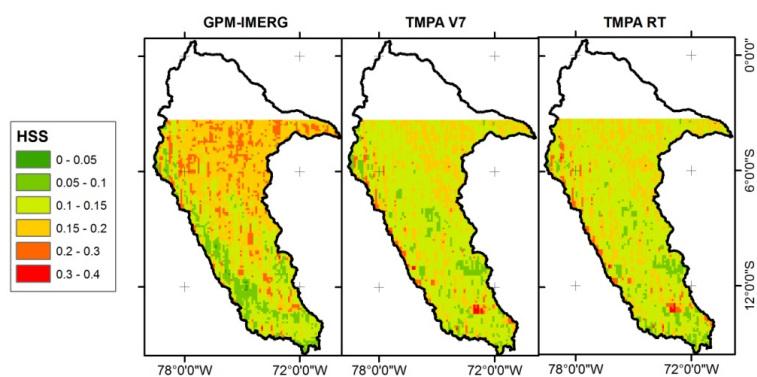
**Figure S1.** a) Relationship between altitude (m asl) and the observed and interpolated (kriging) annual rainfall (mm) for the 181 stations of the Peruvian and Ecuadorian Amazon basin for the 2014-2015 period.





Con formato: Fuente:10 pt, Color de fuente: Texto  
 1

**Figure S2.** Regression line between the observed annual rainfall in 181 rainfall stations (OR) and annual rainfall obtained from a) interpolation (PLU), b) GPM-IMERG, c) TMPA V7, d) TMPA RT for the 2014-2015 period.



Con formato: Fuente:(Predeterminado)  
 NimbusSanL-Regu, Color de fuente: Texto 1

**Figure S3.** Spatial variability of the Heidke Skill Score from a) GPM-IMERG, b) TMPA V7 and c) TMPA RT against PLU ground observation, *period from 2014 to 2015.*

<b>Página 24: [1] Con formato</b>	<b>Ricardo Zubieta Barragàn</b>	<b>6/03/17 18:14</b>
-----------------------------------	---------------------------------	----------------------

Fuente:Sin Cursiva, Color de fuente: Texto 1

<b>Página 24: [1] Con formato</b>	<b>Ricardo Zubieta Barragàn</b>	<b>6/03/17 18:14</b>
-----------------------------------	---------------------------------	----------------------

Fuente:Sin Cursiva, Color de fuente: Texto 1

<b>Página 24: [2] Con formato</b>	<b>Ricardo Zubieta Barragàn</b>	<b>6/03/17 18:14</b>
-----------------------------------	---------------------------------	----------------------

Color de fuente: Texto 1

<b>Página 24: [3] Con formato</b>	<b>Ricardo Zubieta Barragàn</b>	<b>6/03/17 18:14</b>
-----------------------------------	---------------------------------	----------------------

Color de fuente: Texto 1

<b>Página 24: [4] Con formato</b>	<b>Ricardo Zubieta Barragàn</b>	<b>6/03/17 18:14</b>
-----------------------------------	---------------------------------	----------------------

Color de fuente: Texto 1

<b>Página 24: [5] Con formato</b>	<b>Ricardo Zubieta Barragàn</b>	<b>6/03/17 18:14</b>
-----------------------------------	---------------------------------	----------------------

Color de fuente: Texto 1

<b>Página 24: [6] Con formato</b>	<b>Ricardo Zubieta Barragàn</b>	<b>6/03/17 18:14</b>
-----------------------------------	---------------------------------	----------------------

Color de fuente: Texto 1

<b>Página 24: [7] Con formato</b>	<b>Ricardo Zubieta Barragàn</b>	<b>6/03/17 18:14</b>
-----------------------------------	---------------------------------	----------------------

Color de fuente: Texto 1

<b>Página 24: [8] Con formato</b>	<b>Ricardo Zubieta Barragàn</b>	<b>6/03/17 18:14</b>
-----------------------------------	---------------------------------	----------------------

Color de fuente: Texto 1

<b>Página 24: [9] Con formato</b>	<b>Ricardo Zubieta Barragàn</b>	<b>6/03/17 18:14</b>
-----------------------------------	---------------------------------	----------------------

Color de fuente: Texto 1

<b>Página 24: [10] Con formato</b>	<b>Ricardo Zubieta Barragàn</b>	<b>6/03/17 18:14</b>
------------------------------------	---------------------------------	----------------------

Color de fuente: Texto 1

<b>Página 24: [11] Con formato</b>	<b>Ricardo Zubieta Barragàn</b>	<b>6/03/17 18:14</b>
------------------------------------	---------------------------------	----------------------

Color de fuente: Texto 1

<b>Página 24: [12] Con formato</b>	<b>Ricardo Zubieta Barragàn</b>	<b>6/03/17 18:14</b>
------------------------------------	---------------------------------	----------------------

Color de fuente: Texto 1

<b>Página 24: [13] Con formato</b>	<b>Ricardo Zubieta Barragàn</b>	<b>6/03/17 18:14</b>
------------------------------------	---------------------------------	----------------------

Color de fuente: Texto 1

<b>Página 24: [13] Con formato</b>	<b>Ricardo Zubieta Barragàn</b>	<b>6/03/17 18:14</b>
------------------------------------	---------------------------------	----------------------

Color de fuente: Texto 1

<b>Página 24: [14] Con formato</b>	<b>Ricardo Zubieta Barragàn</b>	<b>6/03/17 18:14</b>
------------------------------------	---------------------------------	----------------------

Color de fuente: Texto 1

<b>Página 24: [15] Con formato</b>	<b>Ricardo Zubieta Barragàn</b>	<b>6/03/17 18:14</b>
------------------------------------	---------------------------------	----------------------

Color de fuente: Texto 1

<b>Página 24: [16] Eliminado</b>	<b>Ricardo Zubieta Barragàn</b>	<b>6/03/17 18:14</b>
----------------------------------	---------------------------------	----------------------

estimation every three hours [Schwaller and Morris, 2011]. Recent studies highlight that the GPM

<b>Página 24: [17] Con formato</b>	<b>Ricardo Zubieta Barragàn</b>	<b>6/03/17 18:14</b>
------------------------------------	---------------------------------	----------------------

Color de fuente: Texto 1

<b>Página 24: [17] Con formato</b>	<b>Ricardo Zubieta Barragàn</b>	<b>6/03/17 18:14</b>
------------------------------------	---------------------------------	----------------------

Color de fuente: Texto 1

<b>Página 24: [17] Con formato</b>	<b>Ricardo Zubieta Barragàn</b>	<b>6/03/17 18:14</b>
------------------------------------	---------------------------------	----------------------

Color de fuente: Texto 1

<b>Página 24: [18] Con formato</b>	<b>Ricardo Zubieta Barragàn</b>	<b>6/03/17 18:14</b>
------------------------------------	---------------------------------	----------------------

Color de fuente: Texto 1

<b>Página 24: [19] Con formato</b>	<b>Ricardo Zubieta Barragàn</b>	<b>6/03/17 18:14</b>
------------------------------------	---------------------------------	----------------------

Color de fuente: Texto 1

<b>Página 24: [20] Con formato</b>	<b>Ricardo Zubieta Barragàn</b>	<b>6/03/17 18:14</b>
------------------------------------	---------------------------------	----------------------

Color de fuente: Texto 1

<b>Página 24: [21] Con formato</b>	<b>Ricardo Zubieta Barragàn</b>	<b>6/03/17 18:14</b>
------------------------------------	---------------------------------	----------------------

Color de fuente: Texto 1

<b>Página 24: [22] Con formato</b>	<b>Ricardo Zubieta Barragàn</b>	<b>6/03/17 18:14</b>
------------------------------------	---------------------------------	----------------------

Color de fuente: Texto 1

<b>Página 24: [23] Con formato</b>	<b>Ricardo Zubieta Barragàn</b>	<b>6/03/17 18:14</b>
------------------------------------	---------------------------------	----------------------

Color de fuente: Texto 1

<b>Página 24: [24] Con formato</b>	<b>Ricardo Zubieta Barragàn</b>	<b>6/03/17 18:14</b>
------------------------------------	---------------------------------	----------------------

Color de fuente: Texto 1

<b>Página 24: [25] Eliminado</b>	<b>Ricardo Zubieta Barragàn</b>	<b>6/03/17 18:14</b>
----------------------------------	---------------------------------	----------------------

products). For comparison with satellite estimations,

<b>Página 24: [26] Con formato</b>	<b>Ricardo Zubieta Barragàn</b>	<b>6/03/17 18:14</b>
------------------------------------	---------------------------------	----------------------

Fuente de párrafo predeter.,Color de fuente: Texto 1, español

<b>Página 24: [26] Con formato</b>	<b>Ricardo Zubieta Barragàn</b>	<b>6/03/17 18:14</b>
------------------------------------	---------------------------------	----------------------

Fuente de párrafo predeter.,Color de fuente: Texto 1, español

<b>Página 24: [27] Con formato</b>	<b>Ricardo Zubieta Barragàn</b>	<b>6/03/17 18:14</b>
------------------------------------	---------------------------------	----------------------

Color de fuente: Texto 1

<b>Página 24: [27] Con formato</b>	<b>Ricardo Zubieta Barragàn</b>	<b>6/03/17 18:14</b>
------------------------------------	---------------------------------	----------------------

Color de fuente: Texto 1

<b>Página 24: [28] Con formato</b>	<b>Ricardo Zubieta Barragàn</b>	<b>6/03/17 18:14</b>
------------------------------------	---------------------------------	----------------------

Color de fuente: Texto 1

<b>Página 24: [29] Con formato</b>	<b>Ricardo Zubieta Barragàn</b>	<b>6/03/17 18:14</b>
------------------------------------	---------------------------------	----------------------

Color de fuente: Texto 1

<b>Página 28: [30] Con formato</b>	<b>Ricardo Zubieta Barragàn</b>	<b>6/03/17 18:14</b>
------------------------------------	---------------------------------	----------------------

Color de fuente: Texto 1, Inglés (americano)

<b>Página 28: [30] Con formato</b>	<b>Ricardo Zubieta Barragàn</b>	<b>6/03/17 18:14</b>
------------------------------------	---------------------------------	----------------------

Color de fuente: Texto 1, Inglés (americano)

<b>Página 28: [30] Con formato</b>	<b>Ricardo Zubieta Barragàn</b>	<b>6/03/17 18:14</b>
------------------------------------	---------------------------------	----------------------

Color de fuente: Texto 1, Inglés (americano)

<b>Página 28: [30] Con formato</b>	<b>Ricardo Zubieta Barragàn</b>	<b>6/03/17 18:14</b>
------------------------------------	---------------------------------	----------------------

Color de fuente: Texto 1, Inglés (americano)

<b>Página 28: [30] Con formato</b>	<b>Ricardo Zubieta Barragàn</b>	<b>6/03/17 18:14</b>
------------------------------------	---------------------------------	----------------------

Color de fuente: Texto 1, Inglés (americano)

<b>Página 28: [30] Con formato</b>	<b>Ricardo Zubieta Barragàn</b>	<b>6/03/17 18:14</b>
------------------------------------	---------------------------------	----------------------

Color de fuente: Texto 1, Inglés (americano)

**Página 28: [30] Con formato Ricardo Zubieta Barragàn 6/03/17 18:14**

Color de fuente: Texto 1, Inglés (americano)

**Página 28: [30] Con formato Ricardo Zubieta Barragàn 6/03/17 18:14**

Color de fuente: Texto 1, Inglés (americano)

**Página 28: [30] Con formato Ricardo Zubieta Barragàn 6/03/17 18:14**

Color de fuente: Texto 1, Inglés (americano)

**Página 28: [30] Con formato Ricardo Zubieta Barragàn 6/03/17 18:14**

Color de fuente: Texto 1, Inglés (americano)

**Página 28: [30] Con formato Ricardo Zubieta Barragàn 6/03/17 18:14**

Color de fuente: Texto 1, Inglés (americano)

**Página 28: [30] Con formato Ricardo Zubieta Barragàn 6/03/17 18:14**

Color de fuente: Texto 1, Inglés (americano)

**Página 28: [30] Con formato Ricardo Zubieta Barragàn 6/03/17 18:14**

Color de fuente: Texto 1, Inglés (americano)

**Página 28: [30] Con formato Ricardo Zubieta Barragàn 6/03/17 18:14**

Color de fuente: Texto 1, Inglés (americano)

**Página 28: [30] Con formato Ricardo Zubieta Barragàn 6/03/17 18:14**

Color de fuente: Texto 1, Inglés (americano)

**Página 28: [30] Con formato Ricardo Zubieta Barragàn 6/03/17 18:14**

Color de fuente: Texto 1, Inglés (americano)

**Página 28: [30] Con formato Ricardo Zubieta Barragàn 6/03/17 18:14**

Color de fuente: Texto 1, Inglés (americano)

**Página 28: [30] Con formato Ricardo Zubieta Barragàn 6/03/17 18:14**

Color de fuente: Texto 1, Inglés (americano)

**Página 28: [30] Con formato Ricardo Zubieta Barragàn 6/03/17 18:14**

Color de fuente: Texto 1, Inglés (americano)

<b>Página 28: [31] Con formato</b>	<b>Ricardo Zubieta Barragàn</b>	<b>6/03/17 18:14</b>
------------------------------------	---------------------------------	----------------------

Fuente:Color de fuente: Texto 1, Inglés (americano)

<b>Página 28: [31] Con formato</b>	<b>Ricardo Zubieta Barragàn</b>	<b>6/03/17 18:14</b>
------------------------------------	---------------------------------	----------------------

Fuente:Color de fuente: Texto 1, Inglés (americano)

<b>Página 28: [31] Con formato</b>	<b>Ricardo Zubieta Barragàn</b>	<b>6/03/17 18:14</b>
------------------------------------	---------------------------------	----------------------

Fuente:Color de fuente: Texto 1, Inglés (americano)

<b>Página 28: [31] Con formato</b>	<b>Ricardo Zubieta Barragàn</b>	<b>6/03/17 18:14</b>
------------------------------------	---------------------------------	----------------------

Fuente:Color de fuente: Texto 1, Inglés (americano)

<b>Página 28: [31] Con formato</b>	<b>Ricardo Zubieta Barragàn</b>	<b>6/03/17 18:14</b>
------------------------------------	---------------------------------	----------------------

Fuente:Color de fuente: Texto 1, Inglés (americano)

<b>Página 28: [31] Con formato</b>	<b>Ricardo Zubieta Barragàn</b>	<b>6/03/17 18:14</b>
------------------------------------	---------------------------------	----------------------

Fuente:Color de fuente: Texto 1, Inglés (americano)

<b>Página 28: [31] Con formato</b>	<b>Ricardo Zubieta Barragàn</b>	<b>6/03/17 18:14</b>
------------------------------------	---------------------------------	----------------------

Fuente:Color de fuente: Texto 1, Inglés (americano)

<b>Página 28: [31] Con formato</b>	<b>Ricardo Zubieta Barragàn</b>	<b>6/03/17 18:14</b>
------------------------------------	---------------------------------	----------------------

Fuente:Color de fuente: Texto 1, Inglés (americano)

<b>Página 28: [31] Con formato</b>	<b>Ricardo Zubieta Barragàn</b>	<b>6/03/17 18:14</b>
------------------------------------	---------------------------------	----------------------

Fuente:Color de fuente: Texto 1, Inglés (americano)

<b>Página 28: [31] Con formato</b>	<b>Ricardo Zubieta Barragàn</b>	<b>6/03/17 18:14</b>
------------------------------------	---------------------------------	----------------------

Fuente:Color de fuente: Texto 1, Inglés (americano)

<b>Página 28: [31] Con formato</b>	<b>Ricardo Zubieta Barragàn</b>	<b>6/03/17 18:14</b>
------------------------------------	---------------------------------	----------------------

Fuente:Color de fuente: Texto 1, Inglés (americano)

<b>Página 31: [32] Eliminado</b>	<b>Ricardo Zubieta Barragàn</b>	<b>6/03/17 18:14</b>
----------------------------------	---------------------------------	----------------------

## 4.2 Streamflow simulation

In order to

<b>Página 40: [33] Eliminado</b>	<b>Ricardo Zubieta Barragàn</b>	<b>6/03/17 18:14</b>
----------------------------------	---------------------------------	----------------------

